Atmos. Meas. Tech. Discuss., https://doi.org/10.5194/amt-2018-191
Manuscript under review for journal Atmos. Meas. Tech.
Discussion started: 10 July 2018


Atmospheric Measurement Techniques Discussions

# The Fifth International Workshop on Ice Nucleation phase 2 (FIN-02): Laboratory intercomparison of ice nucleation measurements

DeMott, Paul J.[1], Ottmar Möhler[2], Daniel J. Cziczo[3,4], Naruki Hiranuma[2,a], Markus D. Petters[5], Sarah S. Petters[5,b], Franco Belosi[6], Heinz G. Bingemer[7], Sarah D. Brooks[8], Carsten Budke[9], Monika Burkert-Kohn[10], Kristen N. Collier[8], Anja Danielczok[7,c], Oliver Eppers[11], Laura Felgitsch[12], Sarvesh Garimella[3,d], Hinrich Grothe[12], Paul Herenz[13], Thomas C. J. Hill[1], Kristina Höhler[2], Zamin A. Kanji[10], Alexei Kiselev[2], Thomas Koop[9], Thomas B. Kristensen[13,e], Konstantin Krüger[7,2], Gourihar Kulkarni[14], Ezra J. T. Levin[1], Benjamin J. Murray[15], Alessia Nicosia[6,f], Daniel O'Sullivan[15], Andreas Peckaus[2,g], Michael J. Polen[16], Hannah C. Price[15,h], Naama Reicher[17], Daniel A. Rothenberg[3], Yinon Rudich[17], Gianni Santachiara[6], Thea Schiebel[2], Jann Schrod[7], Teresa M. Seifried[12], Frank Stratmann[13], Ryan C. Sullivan[16], Kaitlyn J. Suski[1,i], Miklós Szakáll[11], Hans P. Taylor[5], Romy Ullrich[2], Jesús Vergara-Temprado[15,10], Robert Wagner[2], Thomas F. Whale[15], Daniel Weber[7], André Welti[13,j], Theodore W. Wilson[15,k], Martin J. Wolf[3], and Jake Zenker[8]

[1]Department of Atmospheric Science, Colorado State University, Fort Collins, CO 80523-1371, USA
[2]Karlsruhe Institute of Technology (KIT), Institute of Meteorology and Climate Research (IMK-AAF), Eggenstein-Leopoldshafen, Germany
[3] Department of Earth, Atmospheric and Planetary Sciences, Massachusetts Institute of Technology, Cambridge, MA, USA
[4]Department of Civil and Environmental Engineering, Massachusetts Institute of Technology, Cambridge, MA, USA
[5]Department of Marine, Earth and Atmospheric Sciences, North Carolina State University, Raleigh, NC, USA
[6]Institute of Atmospheric Sciences and Climate (ISAC-CNR), Bologna, Italy
[7]Institute for Atmospheric and Environmental Sciences, Goethe-University Frankfurt, 60438 Frankfurt am Main, Germany
[8]Department of Atmospheric Sciences, Texas A&M University, College Station, TX, USA
[9]Faculty of Chemistry, Bielefeld University, Bielefeld, Germany
[10]Institute for Atmospheric and Climate Science, ETH Zurich, Zurich, Switzerland
[11]Institute for Atmospheric Physics, Johannes Gutenberg University, Mainz, Germany
[12]Institute of Materials Chemistry, TU Wien, Vienna, Austria
[13]Leibniz Institute for Tropospheric Research, 04318 Leipzig, Germany
[14]Atmospheric Sciences and Global Change Division, Pacific Northwest National Laboratory, Richland, WA, USA
[15]Institute for Climate and Atmospheric Science, School of Earth and Environment, University of Leeds, Woodhouse Lane, Leeds, LS2 9JT, UK
[16]Center for Atmospheric Particle Studies, Carnegie Mellon University, Pittsburgh, PA, USA
[17]Department of Earth and Planetary Sciences, Weizmann Institute, Rehovot 76100, Israel
[a]now at: Department of Life, Earth and Environmental Sciences, West Texas A&M University, Canyon, TX, USA
[b]now at: Department of Environmental Sciences and Engineering, Chapel Hill, NC, USA
[c]now at: German Weather Service, Satellite-based Climate Monitoring, 63067 Offenbach am Main, Germany
[d]now at: ACME AtronOmatic, LLC, Portland, OR, USA
[e]now at: Division of Nuclear Physics, Lund University, Box 118, Lund SE-22100, Sweden
[f]now at: Laboratoire de Météorologie Physique (Lamp-CNRS), Aubière, France
[g]now at German Aerospace Center (DLR), Institute of Technical Physics, 70569 Stuttgart, Germany
[h]now at Facility for Airborne Atmospheric Measurements, Cranfield, MK43 0AL, UK
[i]now at: Pacific Northwest National Laboratory, Richland, WA, USA
[j]now at: Finnish Meteorological Institute, FI-00101 Helsinki, Finland
[k]now at Owlstone Medical Ltd., 162 Cambridge Science Park, Milton Road, Cambridge, CB4 0GH, UK

Atmos. Meas. Tech. Discuss., https://doi.org/10.5194/amt-2018-191
Manuscript under review for journal Atmos. Meas. Tech.
Discussion started: 10 July 2018


Atmospheric Measurement Techniques Discussions

*Correspondence to*: Paul J. DeMott (Paul.Demott@colostate.edu)

**Abstract.** The second phase of the Fifth International Ice Nucleation Workshop (FIN-02) involved the gathering of a large number of researchers at the Karlsruhe Institute of Technology's Aerosol Interactions and Dynamics of the Atmosphere (AIDA) facility to promote characterization and understanding of ice nucleation measurements made by the variety of methods used worldwide. Compared to the previous workshop in 2007, participation was doubled, reflecting a vibrant research area. Experimental methods involved sampling of aerosol particles by online ice nucleation measuring systems from the same volume of air in separate experiments using different ice nucleating particle (INP) types, and collections of aerosol particle samples onto filters or into liquid for sharing amongst offline measurement techniques. In this manner, any errors introduced by differences in generation methods when samples are shared across laboratories were mitigated. Furthermore, as much as possible, aerosol particle size distribution was controlled so that the size limitations of different methods were minimized. The results presented here use data from the workshop to assess the comparability of offline immersion freezing measurement methods activating INPs in bulk suspensions, offline methods that activate INPs in condensation and/or immersion freezing modes as single particles on a substrate, online continuous flow diffusion chambers (CFDCs) operating well above water saturation to maximize immersion and subsequent freezing of aerosol particles, and expansion cloud chamber simulations in which liquid cloud droplets were first activated on aerosol particles prior to freezing. The AIDA expansion chamber measurements are expected to be the closest representation to INP activation in atmospheric cloud parcels in these comparisons, due to exposing particles freely to adiabatic cooling.

The different particle types used as INPs included the minerals illite NX and K-feldspar, two natural soil dusts representative of arable sandy loam (Argentina) and highly erodible sandy dryland (Tunisia) soils, respectively, and a bacterial INP (Snomax®). Considered together, the agreement among offline immersion freezing measurements of the numbers and fractions of particles active at different temperatures following bulk collection of particles into liquid was excellent, with possible temperature uncertainties inferred to be a key factor in determining INP uncertainties. Collection onto filters versus directly into liquid in impingers made little difference. For offline methods that activated single particles on a substrate at a controlled humidity at or above water saturation, agreement with immersion freezing methods was good in most cases, but was biased low in a few others for reasons that have not been resolved, but could relate to water vapor competition effects. Amongst CFDC-style instruments, various factors requiring (variable) higher supersaturations to achieve equivalent immersion freezing activation dominate the uncertainty between these measurements, and for comparison with bulk immersion freezing methods. When operated above water saturation to include assessment of immersion freezing, CFDC measurements often measured at or above the upper bound of immersion freezing device measurements, but often underestimated INP concentration in comparison to an immersion freezing method that first activates all particles into liquid droplets prior to cooling (the PIMCA-PINC device), and typically slightly underestimated INP number concentrations in comparison to cloud parcel expansions in the AIDA chamber; this can be largely mitigated when it is possible to raise the relative humidity to sufficiently high values in the CFDCs, although this is not always possible operationally.

Correspondence of measurements of INPs among online and offline systems varied depending on the INP type. Agreement was best for Snomax® particles in the temperature regime colder than -10°C, where their ice nucleation

Atmos. Meas. Tech. Discuss., https://doi.org/10.5194/amt-2018-191
Manuscript under review for journal Atmos. Meas. Tech.
Discussion started: 10 July 2018


Atmospheric Measurement Techniques Discussions

activity is nearly maximized and changes very little with temperature. At warmer than -10°C, Snomax® INP measurements (all via freezing of suspensions) demonstrated discrepancies consistent with previous reports of the instability of its protein aggregates that appear to make it less suitable as a calibration INP at these temperatures. For Argentinian soil dust particles, there was excellent agreement across online and offline methods; measures ranged within one order of magnitude for INP number concentrations, active fractions and calculated active site densities over a 25 to 30°C range and 5 to 8 orders of corresponding magnitude change in number concentrations. This was also the case for all temperatures warmer than -25°C in Tunisian dust experiments. In contrast, discrepancies in measurements of INP concentrations or active site densities exceeded two orders of magnitude across a broad temperature range for illite NX, and divergent activation spectra between online and offline measurements found at warmer than -25°C in a previous study were replicated. Discrepancies also exceeded two orders of magnitude at temperatures of -20 to -25°C for K-feldspar, but these coincided with the range of temperatures where INP concentrations increase rapidly at approximately an order of magnitude per 2°C cooling for K-feldspar.

These few discrepancies did not outweigh the overall positive outcomes of the workshop activity, nor the future utility of this data set or future similar efforts for resolving remaining measurement issues. Measurements of the same materials were repeatable over the time of the workshop and demonstrated strong consistency with prior studies, as reflected by agreement of data broadly with parameterizations of different specific or general (e.g., soil dust) aerosol types. The divergent measurements of the INP activity of illite NX by online and offline methods was not repeated for other particle types, and the Snomax® data demonstrated that, at least for a biological INP type, there is no expected measurement bias between bulk offline versus online freezing methods to as warm as -10°C. Since particle size ranges were limited for this workshop, it can be expected that for atmospheric populations of INPs, measurement discrepancies will appear due to the different capabilities of methods for sampling the full aerosol size distribution, or due to limitations on achieving sufficient water supersaturations to fully capture immersion freezing in online instruments. Overall, this workshop presents an improved picture of present capabilities for measuring INPs than in past workshops, and provides direction toward addressing remaining measurement issues.

## 1 Introduction

Ice nucleating particles (INPs) are relatively rare atmospheric particles that play a large role in affecting cold cloud properties and precipitation processes. Their presence is needed to initiate ice crystal formation in the absence of conditions that would favor homogeneous freezing nucleation. They are needed as a trigger even in cases where secondary ice formation may be expected to occur. Their varied loading may influence cloud lifetime positively or negatively, as well as impact precipitation rates in mixed phase clouds (e.g., Tan et al., 2016; Fan et al., 2017). Furthermore, the efficacy of different aerosol types as INPs vary greatly, and this is not well resolved for major or minor atmospheric aerosol populations. There is a tremendous need to measure and constrain atmospheric INP populations, and to parameterize these for use in numerical models of all scales, where greatly simplified assumptions on ice phase transitions in clouds are presently used or are thought to be necessary for computational reasons. Studies of INPs occur in laboratory settings where high aerosol loadings are possible, but also in field scenarios where the low number concentrations of INPs challenge near real-time samplers and require larger bulk collections to attempt to



quantify INPs at modest supercooling. Consequently, a variety of devices exists, and the development and use of different instruments continues to expand during a period of great growth in research on mixed phase and ice cloud processes (DeMott et al., 2011). For these reasons, a series of workshops was convened in 2014 to 2015, continuing the historical efforts of the international ice nucleation community to compare and contrast measurements, both to advance understanding within the community and to offer an assessment to the user communities of capabilities and present uncertainties of measurements being published independently.

The philosophy, three-phase nature, and general overview of the Fifth International Ice Nucleation Workshop, dubbed FIN, will be provided in a separate publication in preparation. This paper describes the goals and objectives, and some detailed results from the second phase of FIN, known as FIN-02, focused around comparing ice nucleation measurement systems in laboratory studies of known INPs. A related paper in preparation will describe the separate but integrated activity of comparing these same instrument systems in so-called "blind" experiments. We will describe herein the justification for and distinction of those studies only.

The FIN-02 workshop was held at the Aerosol Interactions and Dynamics in the Atmosphere (AIDA) facility at Karlsruhe Institute of Technology, Eggenstein-Leopoldshafen, Germany during March 2015. FIN-02 was designed to be in the classical form of an ice nucleation workshop, from the standpoint of having a legacy in similar workshops dating back to the late 1960s, as discussed in relation to the 2007 International Workshop on Comparing Ice Nucleation Measuring Systems (ICIS-2007) (unofficially the Fourth International Workshop on Ice Nuclei) by DeMott et al. (2011). The impetus for continuation of the ice nucleation workshop concept was given in that paper. Significant additional developments have occurred in the field of ice nucleation measurements since the time of the 4$^{th}$ workshop, including widespread participation from a global community of researchers and a commercialization development of an online INP measurement system. The FIN-02 workshop was held at the AIDA facility to take advantage of the 4$^{th}$ workshop experience, also held there, and to once again align other measurements with experiments in the AIDA cloud chamber as a mimic of ice nucleation within atmospheric adiabatic cloud parcels.

The goals and objectives of FIN-02 were to:

1) Compare ice nucleation measurement systems for conditions considered to be equivalent as much as possible, across a wide dynamic temperature range, including temperatures warmer than -15°C.

2) Gain insights into how detection of ice nucleation is influenced by the specific configuration of similar measurement systems.

3) Gain insights into the strengths and weaknesses, limits of detection, potential artifacts and other peculiarities of different INP detection systems.

4) Utilize different INP types to investigate if differences between instruments vary with these different types.

## 2 Methods

Guided by the objectives of FIN-02 and the variety of current systems available for measuring INPs, two broad categories of portable ice nucleation instruments were defined for studies. These categories are, firstly, instruments operating online and, secondly, those utilizing collections of particles for subsequent offline processing. This categorization to a large extent also separates methods that sample "dry" particles and those that utilize "wet"

Atmos. Meas. Tech. Discuss., https://doi.org/10.5194/amt-2018-191
Manuscript under review for journal Atmos. Meas. Tech.
Discussion started: 10 July 2018




suspensions of particles in liquid for assessing freezing properties, with a few exceptions we will note. Methods for sampling particles from a dry state permit assessment of the action of a variety of ice nucleation mechanisms that occur in different water relative humidity ($RH_w$) regimes: deposition nucleation primarily occurring below water saturation, and condensation and immersion freezing on approaching or exceeding water saturation, where cloud droplet activation occurs. Wet suspension experiments isolate the action of immersion freezing nucleation, and certain methods isolate immersion freezing for single aerosol particles (Burkert-Kohn et al., 2017). No measurements of contact freezing were included in this study, and neither will we discuss results herein from workshop measurements that were made in the regime associated with deposition nucleation (including at homogeneous freezing temperatures), but we will focus on inter-comparisons of particles acting via immersion freezing or proximal behaviors. By proximal behaviors, we follow the terminology of Vali et al. (2015), wherein condensation freezing is not necessarily considered as distinguishable from immersion freezing, and, hence, online diffusion chambers measuring in the regime well above water saturation are considered to be able to approximate more direct measurements of immersion freezing.

The number of ice nucleation measurement systems participating in FIN-02 was slightly more than twice the number that participated in the 4th workshop in 2007, reflecting a similar increase in the number of researchers now operating in this field. There were 21 total systems represented in FIN-02, 9 online and 11 offline, plus the AIDA chamber. Names and basic descriptions are provided in Tables 1 and 2 and operational principles are given in the Supplement to this paper. Shorthand names of instruments are defined in the manuscript at first introduction. The thermodynamic trajectories used by the primary instrument types used in FIN-02 are shown in Fig. 1 and their basic manners of operation are discussed in the following section.

### 2.1 Online (portable) systems

Online or continuous flow systems were represented primarily in the form of continuous flow ice-thermal diffusion chambers that sample initially dry particles and expose these to conditions leading to ice nucleation. Amongst these were portable chambers with cylindrical (e.g., Rogers et al., 1988) and parallel plate (e.g., Stetzer et al., 2008) wall systems. The former included the Colorado State University continuous flow diffusion chamber (CFDC-CSU) and systems descendant from this design: the Texas A&M continuous flow diffusion chamber (CFDC-TAMU) and the Ice Nucleation Instrument of the Karlsruhe Institute of Technology (INKA). In all of these, a cylindrical aerosol lamina representing a minor portion of the total flow is constrained within particle-free sheath flows (top to bottom) between two cylindrical walls that are ice-coated and can be independently temperature-controlled to determine the $RH_w$ and temperature at the center of the aerosol lamina in upper "growth" regions of the chambers. Parallel plate systems insert the downward-flowing aerosol lamina between sheath flows inside two parallel rectangular ice-coated plates to similarly expose particles to controlled temperature and humidity conditions in their growth sections. Parallel plate devices of quite common design included in FIN-02 were the ETH-Zurich Portable Ice Nucleation Chamber (PINC), the Pacific Northwest National Laboratory Compact Ice Chamber (CIC-PNNL), and the Droplet Measurement Technologies SPectrometer for Ice Nucleation (SPIN) devices operated by groups from the Massachusetts Institute of Technology (SPIN-MIT) and the Leibniz Institute for Tropospheric Research (SPIN-TROPOS).

Atmos. Meas. Tech. Discuss., https://doi.org/10.5194/amt-2018-191
Manuscript under review for journal Atmos. Meas. Tech.
Discussion started: 10 July 2018


Atmospheric Measurement Techniques Discussions

Measurements from continuous flow diffusion chambers are represented by the red lines in Fig. 1. All of the continuous flow diffusion chambers have the ability to raise the $RH_w$ above the water saturation line in order to investigate ice nucleation during or following condensation of water droplets. Once water droplets have formed, a means is required to discriminate ice particles from water droplets. The most common method used for phase discrimination in continuous flow chambers is to selectively shrink activated liquid droplets to accentuate ice crystals by their larger optical size. Some instruments use laser light depolarization for phase discrimination, but this is typically a suitable method only for higher signal to noise situations and ice active fractions that exceed several percent of particles (Nicolet et al., 2010; Garimella et al., 2016; Zenker et al., 2017). For these reasons, all such devices in FIN-02 include an "evaporation" section as a shorter column length below their growth sections, where the $RH_w$ is lowered toward ice saturation conditions by setting the two wall temperatures to be equivalent at either the warmest wall, coldest wall, or lamina temperature in the growth sections (see Supplement). When the temperature gradient in the growth section is adjusted to generate water supersaturated conditions that activate cloud droplets within the aerosol lamina, the lower $RH_w$ in the evaporation section shrinks droplets back toward haze particle sizes. This method works up to some high value of $RH_w$ whereupon activated cloud droplets survive through to detection, often referred to as the water droplet breakthrough $RH_w$. The $RH_w$ at which this occurs varies with temperature, geometry and flow rate for different devices. Therefore, a single $RH_w$ level for this condition to occur is not noted in Fig. 1, and why results will be given at certain specific $RH_w$ values (or % supersaturation values, which equal $RH_w$-100) for some instruments or experiments and at the maximum $RH_w$ achievable at other times. We did not seek to fully document this behavior during FIN-02, and will not seek to understand differences amongst the different continuous flow chambers in this regard within this paper.

While one might be inclined to dismiss $RH_w$ in excess of 102% as irrelevant for most atmospheric situations, there are a number of reasons why higher values are often referenced for continuous flow diffusion chambers. Primarily, continuous flow diffusion chamber instruments in general do not presently expose particles to uniform water supersaturations with the precision currently achieved by cloud condensation nuclei (CCN) instruments. The transition into the immersion freezing regime above water saturation does not occur sharply in line with the supersaturation calculated for the aerosol central lamina, but rather ensues completely only at higher $RH_w$ as controlled by aerosol particle properties and instrument characteristics. For example, hygroscopicity and kinetic factors control water uptake, chambers have different flow rates and growth section lengths, there is a finite difference in $RH_w$ across the aerosol lamina, and many devices appear (for as yet unclear reasons) often to induce a proportion of all particles to escape the defined aerosol lamina and expose these particles to lower $RH_w$ (DeMott et al., 2015; Garimella et al., 2017). Some additional discussion of this point is given later in this paper. The consequence is that when one seeks to represent complete immersion of particles into liquid water and subsequent freezing, then an $RH_w$ nominally greater than 100% is used, sometimes up to the limit before water droplet breakthrough occurs (DeMott et al., 2015). Hence, higher $RH_w$ is used in these instruments to bypass limitations in achieving CCN activation on the entire particle population, and to increase the condensation rate and thus water content of the formed droplets. In this context, instrument $RH_w$ is not used to simulate the cloud supersaturations and time scales that parcels would experience in ascending air masses (as is simulated in the AIDA cloud chamber – see next section). It is also the case that a single



$RH_w$ value may not lead to the same activation fraction of particles in different instruments. This leads to inherent uncertainty in comparing results from these chambers, an issue that we will only acknowledge here, but did not plan as a special focus of study in FIN-02. We suggest that individual instrument teams need to understand these behaviors of their instruments sufficiently and that they be accounted for when performing measurements in the ambient atmosphere. Consequently, decisions on the $RH_w$ value reported for comparison of immersion freezing or proximal behaviors of these instrument systems to other immersion freezing devices was up to each instrument team. While these are the primary comparisons made in this paper, we note that the continuous flow instruments processed dry particle samples by slowly "scanning" $RH_w$ from near ice saturation conditions to water supersaturated conditions (see DeMott et al., 2011 for discussion of these methods, and the Supplement section S.1.2 for a few examples), and these data have been archived from FIN-02. Investigators were then asked to select those data they felt represented the highest (not necessarily maximum) immersion freezing activity it was deemed possible to assess in their $RH_w$ scans, and reported the INP concentrations and $RH_w$ values selected.

For continuous flow diffusion chambers in FIN-02, no additional corrections besides internal losses (if known) were applied. In other words, correction factors to account for the inability to assess maximum activation in the supersaturated regime, as discussed by DeMott et al. (2015), Garimella et al. (2017), and Burkert-Kohn et al. (2017) were not applied. We discuss particle losses in lines feeding various instruments in section 2.4.

Unique among the continuous flow chambers in FIN-02 was the combination of the PIMCA (Portable Immersion Mode Cooling chamber) device in series with the PINC instrument, referred to herein as PIMCA-PINC, wherein droplets are first activated on individual dry particles at temperatures above 0°C prior to cooling during flow into the colder temperature PINC to observe immersion freezing (See Supplement Section S.1.6). This is intended to provide the most explicit simulation of immersion freezing. Experimental trajectories for PIMCA-PINC essentially follow those of offline immersion freezing devices (see below), but activation is on single droplets of reasonably comparable aerosol mass fraction content at all temperatures.

The CIC-PNNL flow diffusion chamber instrument was also operated at times in a non-standard manner to activate droplets at high supersaturation under modest supercooling in its upper chamber region and cool them to immersion freezing in the lower chamber region during FIN-02 studies (Kulkarni et al., 2018), but only data collected in the standard manner of generating near steady-state supersaturation at a single lamina temperature were included in the comparison in this manuscript.

### 2.2 Offline systems

Among instruments that post-processed particle collections in different experiments were diffusion chamber devices that processed particles collected onto substrates and devices that recorded freezing by particles within liquid droplets or confined liquid volumes. Thermal diffusion chamber devices that processed particles on substrates during FIN-02 were the FRIDGE (FRankfurt Ice nucleation Deposition freezinG Experiment) instrument operated to above water saturation in its standard mode, referred to here as FRIDGE-STD (see Supplement section S.2.10), and the DFPC-ISAC (Dynamic Filter Processing Chamber - Institute of Atmospheric Sciences and Climate, National Research Council of Italy) instrument (see Supplement Section S.2.11). These two methods were originally designed to address



the condensation freezing and deposition ice nucleation modes at water saturation and below. However, the uncertain difference between condensation freezing and immersion freezing mechanisms (Vali et al., 2015) argue for an evaluation of both methods by including their results obtained at saturation in this intercomparison. The thermodynamic path of measurements using these instruments is the same as for the continuous flow diffusion chambers in Fig. 1 (red lines), but terminate close to water saturation. For these two instruments, no limitation on condensing water and freezing particle populations is assumed for cases of light particle loading on substrates, as this limits reduction of saturation ratio over the substrates due to growth of some particles as ice. These instrument teams were allowed to evaluate possible influence of water vapor competition on limiting supersaturation over their substrates in each experiment, prior to entering data into comparisons shown herein. Attempts were made to limit particle collections to shorter times that would keep particle loading light on the substrates, but high aerosol concentrations generated for accessing ice active fraction over several orders of magnitude led to some uncertainty in defining appropriate collection times. When the influence of vapor competition on ice nucleation and growth were inferred, experimental results from these diffusion chambers were eliminated from comparisons.

Wet suspension measurements of immersion freezing are depicted in Fig. 1 by the blue arrows. These measurements fall along the water saturation line because collected particles are suspended in pure water whose final water activity is essentially 1. In some cases, the mass and surface area within liquid water volumes is varied over several orders of magnitude of weight percent, via adding purified water for dilution, in order to cover a range of temperatures of activation. The various wet suspension methods used in FIN-02 are listed in Table 2. Details on all of the specific immersion freezing methods are also given in the Supplement to this manuscript. The basic types of methods used involved: 1) cooling arrays of droplets of particle suspensions placed on a cold stage and within oil, as done with the Carnegie Mellon University Cold Stage (CMU-CS) and the Karlsruhe Institute of Technology Cold Stage (KIT-CS); 2) cooling of suspension aliquot volumes in array compartments, as done with the CSU Ice Spectrometer (IS) and the Bielefeld Ice Nucleation ARraY (BINARY); 3) creating and cooling emulsions of particle suspensions as done in the Vienna Optical Droplet Crystallization Analyzer (VODCA) instrument; 4) cooling of droplets containing particles that are pipetted directly onto a coated hydrophobic glass slide, as done with the University of Leeds Microliter Nucleation by Immersed Particles Instrument (μL-NIPI) and the North Carolina State University Cold Stage (NCSU-CS), and using similar droplet arrays on the FRIDGE substrates (referred to as FRIDGE-IMM in this case, for FRIDGE Immersion Freezing); 5) freezing of a droplet train within a microfluidic device WeIzmann Supercooled Droplets Observation on Microarray (WISDOM); 6) and cooling of levitated particles as in the Mainz Acoustic Levitator (M-AL).

Most wet suspension groups shared common samples from collections into liquid water (see discussion of sampling protocol in section 2.4), while in many cases the IS and FRIDGE-IMM measurements involved processing particles re-suspended from filters in pure water. Among the wet suspension measurements, only the μL-NIPI, hereafter simply NIPI, measurements were conducted immediately after collection at KIT, while others processed the samples at their home institutes.

**2.3 AIDA chamber**

Atmos. Meas. Tech. Discuss., https://doi.org/10.5194/amt-2018-191
Manuscript under review for journal Atmos. Meas. Tech.
Discussion started: 10 July 2018




Finally, besides the two basic methods for assessing ice nucleation activity, the 84 $m^3$ AIDA controlled expansion cloud chamber, denoted as AIDA hereafter, was used to perform experiments to form clouds via expansion cooling, serving as a cloud parcel comparison to other measurements. In this regard, we follow the example of the 2007 workshop, and a key recommendation from prior ice nucleation workshops that an expansion cloud chamber be utilized to provide a simulation of cloud activation (DeMott et al., 2011). The thermodynamic path of the AIDA chamber experiments is shown schematically by the yellow curves in Fig. 1. Of note in this regard is the fact that small supersaturations occur prior to cloud formation in AIDA, but once droplets are activated on all particles, then cooling follows at water saturation until a point where evacuation cannot sustain cooling against the surrounding warmer volume, and clouds begin to dissipate. In this regime at water saturation, it needs to be understood again that comparison to continuous flow chambers should not be made for those instruments at water saturation, but only for the higher values that assure more complete droplet activation within their sample lamina. For comparison to immersion freezing results by other methods, we have omitted AIDA experiments for which high ice nucleation rates were achieved at below water saturation (e.g., deposition nucleation regime), and wherein full subsequent activation of particles as CCN was not achieved due to rapid ice growth.

### 2.4 Ice nucleating particles and aerosol generation

A variety of relevant aerosol particle types were produced for FIN-02 studies, as listed in Table 3. These types reflect surrogates for atmospheric mineral dust INPs (illite NX) or their key components (K-feldspar), natural soil dust samples of varied arability collected from different regions of the world (Argentinian soil dust, erodible Tunisian soil dust, Saharan dust), and a biological (microbial, proteinaceous) INP type (Snomax®). These different INPs also span a range of activation temperatures that cover most of the mixed-phase cloud regime (i.e., 0 to -36°C), so they provide a stringent test of measurement capabilities and any biases that may occur.

Aerosol generation methods largely followed those presented in Hiranuma et al. (2015). Particles were independently provided to two different chambers, these being the AIDA chamber and a 4 $m^3$ holding chamber that will be referred to here as the aerosol particle chamber (APC). A total of 27 AIDA and 29 APC experiments were carried out during FIN-02. The particle types used for all 56 experiments are summarized in Table 3. Dry soil and mineral dust particles were generated using a rotating brush disperser (PALAS, RBG1000) and were subsequently passed through a series of inertial cyclone impactor stages (with 50% cut-point diameters of about 5 and 1 μm) prior to introduction into each chamber. This was an important step in limiting the numbers of particles present at sizes above 1 μm and emphasizing mode sizes that could be efficiently sampled by all measurement systems, including continuous flow devices. While natural particle distributions may sometimes include INPs to much larger sizes, it was deemed important for this study to limit this factor that can lead to measurement discrepancies due to sampling limitations. Size distributions of dry particles were measured using a scanning mobility particle sizer (SMPS, TSI Inc., Model 3081 differential mobility analyzer, DMA, and Model 3010 condensation particle counter, CPC) and an aerodynamic particle sizer (APS, TSI Inc., Model 3321). Particles were assumed to be spheres, and dynamic shape factors and particle densities listed in Table 3 were used to obtain the geometric-based (volume equivalent) diameters from the SMPS and APS data (Hiranuma et al., 2014b; 2015). Total particle surface areas were calculated and

Atmos. Meas. Tech. Discuss., https://doi.org/10.5194/amt-2018-191
Manuscript under review for journal Atmos. Meas. Tech.
Discussion started: 10 July 2018


Atmospheric Measurement Techniques Discussions

tabulated as a function of time using lognormal fits to size distributions in each experiment, as shown for two exemplary soil dust experiments (one AIDA and one APC) in Fig. 2.

Wet particle dispersion was used during FIN-02 to generate INPs from Snomax® suspensions. The injection of Snomax® particles into the ventilated APC and AIDA vessels was achieved by atomization of a 5 g Snomax® suspension in 1 L of 18.2 MΩ ultrapure water followed by a diffusion dryer. The home-built atomizer used in Wex et al. (2015) was employed for all Snomax® particle generation. A total of eight polydisperse Snomax® injections were performed during FIN-02 (Table 3). Accordingly, aerosolized Snomax® particles were characterized for total number concentration and size distribution during each experiment.

Due to the efforts made to limit the generation of supermicron particles, the online ice nucleation instruments typically operated without special upstream impactors that would be used during atmospheric sampling to limit aerosol particles entering at sizes that could be mistaken as grown ice crystals (i.e., many CFDCs differentiate ice and aerosols by size alone). However, it was the case in some experiments that larger particles were present and could "pollute" size channels that typically demarcate only ice crystals. Redefinition of ice channels was done in some cases to enable use of data from these experiments. An example of such corrections is given in Supplement Section S.1.2.

An example of a timeline of aerosol particle properties at the start of a typical experimental day is shown in Fig. 3. On most days, a first period involved generation of particles into the APC and the start of sampling for offline measurement systems. The chamber was initially filled with a high concentration of aerosol particles to create appropriate sampling conditions for the offline systems, which typically require high total particle concentration (0.4 < mass concentration< 40 mg $m^{-3}$) in order to take advantage of the ability of some of these methods to assess the lower INP concentrations active at modest supercooling. A total of seven samplers (i.e., DFPC-ISAC filter, NC State particle into liquid impingers – one devoted to the Leeds group, NC State filter, FRIDGE filters, IS filter, and STXM/NEXAFS grids for future study) were employed and ran up to 100 min. It was typical for the NC State and CSU filters to operate over the same time period as the impingers, while the FRIDGE filters were collected over multiple and shorter time periods (10 min). The DFPC-ISAC filters were only collected during sampling from the AIDA chamber, and over periods of 10's of seconds to limit particle loading for steady state chamber measurements. In some cases, aerosol particle concentrations were sufficiently depleted that an additional APC fill was done to augment collections and suffice for the later sampling by online (dry particle) systems. When this was done, the separate impinger samples for each period were combined prior to being divided for distribution and processing by different groups. A smaller injection of aerosol mass and concentration was typically used during the second fill in order to optimize sampling conditions for the online instruments. Offline sampling was suspended for the online sampling period. Such a two-stage injection period is highlighted in Fig. 3 by two regions of blue shading. Smoothed, interpolated aerosol curves are shown in Fig. 3, but exponential fits to decay periods were found to represent particle number concentrations with $r^2$ values exceeding 0.98, as expected for the first order loss processes occurring in the APC during sampling. Curves are shown for total particle numbers, numbers of particles larger than 0.5 μm (only for comparison), and total particle surface area (spherical equivalency assumed for measured particle diameters). By integrating the exponential fit functions during sampling periods (blue shading), the integrated number concentrations and surface areas were determined for the combination of offline sample periods. For example, with reference to Fig.

Atmos. Meas. Tech. Discuss., https://doi.org/10.5194/amt-2018-191
Manuscript under review for journal Atmos. Meas. Tech.
Discussion started: 10 July 2018




3 and the fit to the exponential decay in any period $i$ with start and end times $t_{0i}$ and $t_{1i}$, respectively, the period average total aerosol concentration ($\bar{n}_{CPC,offline,i}$) is given by,

$$\bar{n}_{CPC,offline,i} = \int_{t_{0i}}^{t_{1i}} a_i \exp(b_i\, t) = \frac{a_i}{b_i}(\exp(b_i t_{1i}) - \exp(b_i t_{0i})) \quad (1)$$

Then for $i$ = 1 to x periods of offline sampling of aerosols from the APC for interval times $\Delta t_i$,

$$\bar{n}_{CPC,offline} = \sum_{i=1}^{x} \Delta t_i n_{CPC,offline,i} \,/\, \sum_{i=1}^{x} \Delta t_i \quad (2)$$

Because it was desired as a first inspection to compare as many instruments as possible by INP number concentration measurement alone, INP concentrations measured by online systems during the later period (green shaded area in Fig. 3) at any sample time $t$ were corrected to give equivalence to the volumetric INP concentration measured by offline systems during their integrated sampling periods. That is,

$$n_{INP,online,corr}(t) = n_{INP,online}(t)\, \bar{n}_{CPC,offline}/n_{CPC}(t) \quad (3)$$

Correction factors for the online period were sometimes well in excess of 1 and up to 13 in a few experiments, since online sampling from the APC oftentimes continued for more than a few hours after the offline period had been completed. Comparing online and offline systems during APC sampling as number concentrations per volume of air is considered the most straightforward comparison of equivalence due to requiring no special assumptions. We may note that integrated (spherical equivalent) surface areas for the offline systems are determined in the same manner as reflected in Eqs. 1 to 3 for results shown in Section 3.2.

In addition to APC experiments, the online instruments and a few offline samplers also drew aerosol particles from the AIDA chamber during the afternoon periods of each day. Sampling from AIDA was done in the time prior to the start of cloud expansions. In addition to the aforementioned DFPC-ISAC filter collections, the collection of particles onto wafers for use in the standard (deposition/condensation freezing) FRIDGE instrument processing mode (see Supplement Section 2.10) was also performed from the AIDA chamber for limited time periods, with a similar goal to limit total particle number loading for the diffusion chamber measurements. Aerosol number concentrations were typically much lower in AIDA, and since the total volume of AIDA is much larger, the decay of number concentrations due to sampling by other instruments prior to expansion was much slower than in the APC. Thus, in most cases, comparison measurement from other instruments to the AIDA ice crystal activation results could be made directly, with a small correction at times to account for the higher (in this case) total particle (CPC) number concentrations at the time of sampling versus those during the subsequent AIDA expansion. We compare activated fractions and the deterministic active site density parameter in these experiments so that multiple AIDA sampling experiments of the same aerosol types may be included. This also allows for comparison of selected APC results to AIDA chamber results for similar aerosol types across the entire workshop period. This allows evaluation of measurement consistency, and comparison to previously published parameterizations.

Atmos. Meas. Tech. Discuss., https://doi.org/10.5194/amt-2018-191
Manuscript under review for journal Atmos. Meas. Tech.
Discussion started: 10 July 2018


Atmospheric Measurement Techniques Discussions

We use calculated geometric aerosol surface areas, under the assumption of spherical equivalent diameters, to compute and compare surface active site densities, $n_{s,geo}\ (T)$. Assuming a uniform distribution of $n_{s,geo}\ (T)$ over a given total aerosol surface area ($S_{tot}$) and its size independency, we follow Hiranuma et al. (2015) to approximate $n_{s,geo}\ (T)$ as,

$$n_{s,geo}(T) \approx \frac{n_{INPs}(T)}{S_{tot}} \quad (4)$$

Uncertainty in $n_{s,geo}\ (T)$ is computed in quadrature from the confidence interval data for each INP type and assuming a 25% uncertainty in $S_{tot}$. $S_{tot}$ is computed by normalizing the integrated aerosol surface area ($\mu m^2\ cm^{-3}$) by total particle number concentrations. Integrated surface areas are listed in Table S1 of the Supplement to this manuscript. These are determined based on lognormal fits to the aerosol distribution merged over the full particle size range from aerodynamic and aerosol mobility measurements (Fig. 2). Values of $n_{s,geo}\ (T)$ will be listed and plotted in $m^{-2}$ herein.

All investigators were given the ability to re-evaluate data quality and potential experimental issues after the original archive was produced. The amount of data contributed to final comparisons varied widely amongst the different instruments, in some cases due to operational issues that arose during the workshop. Finally, we note that no corrections for particle losses in sample lines are made for comparisons shown herein. This is due to the fact that these losses may be assumed to be negligible in comparison to other uncertainties as defined by confidence intervals for the measurements. As noted in Fig. 2, both particle number and surface area in these experiments were mainly from particles in the size range between 0.1 and 1 μm. Using the worst-case sampling scenario, which was for the PIMCA-PINC instrument sampling from the AIDA chamber (flow rate of 1.6 L $min^{-1}$ through 5 m of 0.457 cm interior diameter stainless tubing, and assumed bulk particle density of 2.6 g $cm^{-3}$), calculations of estimated penetration efficiency through tubing versus particle size were made using equations from Baron and Willeke (2005). Calculations captured diffusional losses in tubing, inertial losses in a straight tube (i.e., incline was ignored), and impaction losses in tubing (four 90° bends assumed). This demonstrated that penetration efficiency likely exceeded 88% at all sizes below 1 μm, and even at a size of 2 μm, the proximal upper size generated in any experiments, ~60% of the particles should have reached all instruments.

## 3 Results

### 3.1 APC sampling of INPs

As discussed in Section 2, the primary comparison of methods for sampling different INP types from the APC was for the measured or calculated number concentrations of INPs. Four experiments in which most measurement methods sampled from the APC are shown in Figures 4 to 7. These comparisons necessarily exclude the AIDA chamber data. Each figure assesses, 1) comparisons of online (larger blue colored symbols of different types are for the CFDC-CSU, SPIN-TROPOS and SPIN-MIT, CIC-PNNL, INKA and PIMCA-PINC) versus offline instruments (all other symbols

Atmos. Meas. Tech. Discuss., https://doi.org/10.5194/amt-2018-191
Manuscript under review for journal Atmos. Meas. Tech.
Discussion started: 10 July 2018




of various types and colors); 2) comparison of different offline methods, whether immersion freezing arrays on substrates or in aliquots (IS, BINARY, NIPI, KIT-CS, NCSU-CS, CMU-CS, VODCA, FRIDGE-IMM) or microfluidic devices (WISDOM), or in diffusion chambers (FRIDGE-STD) or electrodynamic traps (M-AL); 3) shared (most immersion freezing arrays or devices using the common impinger samples) versus individual samples (IS and FRIDGE-IMM); and 4) different collection methods (filters for IS and FRIDGE-IMM; impingers for others).

The comparisons obtained for sampling Argentinian soil dust particles (Fig. 4) were among the best in this study. A most striking feature of these results is the general correspondence amongst all methods and sampling types, mostly within one order of magnitude in INP number concentrations across the entire mixed phase temperature regime, which is good agreement when put in the perspective of INP number concentration increases of about 7 or more orders of magnitude in this temperature regime from -5 to -35°C. Consistency is seen whether comparing offline methods versus online methods in their temperature range of overlap, within the online and offline categories, within shared offline methods, and whether offline samples are collected by impinger or separate polycarbonate filters (again, IS and FRIDGE-IMM) that were subsequently rinsed of particles. Note that the IS filter was collected simultaneously with the impinger sample, while the FRIDGE-IMM filter was collected over a shorter time frame. Greatest discrepancies, in consideration of measurement uncertainties (see Supplemental) occur at the coldest temperatures. In this region, data from the PIMCA-PINC instrument, which activates individually-grown droplets on particles prior to cooling, falls at the upper end of measured INP concentrations in comparison to the few other immersion methods that extended to the heterogeneous ice nucleation limit, just warmer than homogeneous freezing temperatures. We note again here that some scatter may occur in the online methods due to the imperfect understanding of what value for processing $RH_w$ might represent complete immersion freezing. No correction has been made for this issue, previously discussed by DeMott et al. (2015), Garimella et al. (2017) and Burkert-Kohn et al. (2017), which would drive the online flow chamber data to higher values. Nevertheless, overall, the inter-comparison represented in Fig. 4 is encouraging.

Measurements for a Tunisian desert dust sampling experiment in the APC are shown in Fig. 5. Fewer overall measurements are contained in this comparison. Nevertheless, results are similar to those obtained for the Argentinian soil dust sample, albeit with a slightly higher than one order of magnitude overall range of values measured by all methods at any particular temperature. A somewhat steeper inflection in data near -20°C is noted in this case, which may exacerbate discrepancies between methods due to temperature uncertainties alone. Within the offline immersion freezing methods sharing the impinger sample, variance increases from a factor of a few to more than an order of magnitude at colder temperatures. Two FRIDGE-IMM samples were collected 15 minutes apart for this experiment, and demonstrate results that span the range of INP concentrations measured by all methods at temperatures near -20°C. The two FRIDGE-IMM filter samples also bracket the results from the IS filter collection that spanned the same time frame as the impinger sample. At the coldest temperatures examined, a separation develops between the online (higher) and offline (lower) INP concentration ranges. And as for the Argentinian soil sample, the PIMCA-PINC data cap the online instrument measurements of Tunisian soil dust at the coldest temperatures, leading to nearly a two order of magnitude discrepancy of measured INP concentrations at below -32°C. Thus, this experiment is consistent with the experiment for Argentinian soil dust particles in showing good agreement amongst INP measurements, but with



the largest uncertainties typically occurring at the very warmest and coldest ends of the temperature spectrum, where ice nucleation activity is lowest and highest, respectively.

Although both of the soil dust examples show a sigmoidal ice nucleation activation temperature spectrum, this is more pronounced for the less "desert-like" sample from Argentina. This likely reflects the activity of different sized particles and the presence of multiple INP types or ice active sites, with the warmest freezers possibly from proteinaceous and other heat labile organic INPs achieving a plateau of activation at temperatures warmer than -20°C (see, e.g., O'Sullivan et al., 2014; Hill et al., 2016; Beydoun et al., 2017). This sigmoidal behavior is also seen in the upper bound of precipitation water immersion freezing spectra (Petters and Wright, 2015) and in natural particle samples collected over arable soil regions, where it has been attributed to soil and plant emissions (Delort and Amato, 2018). The levelling-off of the ice nucleating activity at low temperatures is also similar to desert dust laden air observed around Cape Verde (Price et al., 2018).

For the conditions of overlap between online and offline methods (<-20°C), neither of the soil dust examples tested show the types of discrepancies noted for the mineral illite NX (Emersic et al., 2015; Hiranuma et al., 2015; Beydoun et al., 2016). Co-location of instruments, limitation of the size range of particles collected, and sharing of common samples collected at the same time onto filters or into liquid may have all contributed to the consistency of results for natural soil dusts in this study. If true, it does not mean that different methods will agree in atmospheric measurements, but rather that the differences that do occur are influenced by other sampling limitations (e.g., sizes of particles that can be assessed, etc.) (Burkert-Kohn et al., 2017; DeMott et al., 2017). This would also apply to intercomparisons in which laboratories in different places are free to dispense samples independently prior to comparison. Alternatively, or in addition, it may be the case that the soil dusts examined in this study have specific features for activation that differ from minerals or proxy dusts like illite NX, and these are less influenced by water immersion and storage either cool or frozen.

Results for illite NX as a test aerosol will be addressed below in the discussion of sampling experiments directly from AIDA and comparison of all results by active site density. K-feldspar was examined as an additional example of a mineral aerosol in this study. This K-feldspar sample is referred to as FS02, as described in Atkinson et al. (2013) and Peckhaus et al. (2016), and has similar ice nucleating activities to other K-feldspars with microtexture (Whale et al., 2017). Comparison of INP concentrations in Fig. 6 shows similar results as for the soil dust samples, but the INP activation curve of K-feldspar particles is much steeper with a pronounced levelling-off below about -25°C (i.e., it reaches a maximum and is only weakly dependent on temperature). This steepness is associated in this case with an up to two order of magnitude spread among offline immersion freezing methods at around -25°C, greater than for the natural soil dusts at this temperature. This may be partly explained by temperature uncertainties, which range from ±0.2 to ±0.5°C for the immersion freezing methods (see Supplement). Confidence intervals are also seen to be relatively large in this case, probably reflecting the high sensitivity of freezing to temperature. The leveling-off of INP concentrations below -25°C is consistent with previous measurements for K-feldspars summarized in Harrison et al. (2016) and Niedermeier et al. (2015). The separate filter sample (IS and FRIDGE-IMM) results are again consistent with those from instruments that shared the same impinger sample, although falling mostly to the upper side of these other measurements. A potential difference in this case is the time that particles may have spent stored in water, as the

Atmos. Meas. Tech. Discuss., https://doi.org/10.5194/amt-2018-191
Manuscript under review for journal Atmos. Meas. Tech.
Discussion started: 10 July 2018




IS and FRIDGE-IMM results were presumably processed immediately after placing particles into liquid, thus minimizing time for flocculation of the clay. Most online samplers in Fig. 6 show results that are consistent with the upper bounds of offline measurements at below -20°C. Exceptions are the SPIN-MIT instrument data, elevated at -21.3°C, and the PIMCA-PINC data elevated at colder temperatures, as was seen for PIMCA-PINC data in the Argentinian and Tunisian soil dust experiments.

The experiments for soil dusts and minerals do not offer comprehensive comparisons of the consistency of all of the different measurement methods at cloud temperatures warmer than about -20°C. Using a more active INP type within this temperature regime, Snomax® bacterial INPs, offers the opportunity for such assessment, as shown in Fig. 7. The unique activation properties of these INPs suggest separating the discussion around two temperature regions of Fig. 7; for temperatures warmer and colder than about -9°C. Online measurements were only obtained at temperatures colder than -9°C, where the ice nucleation activity is found to be maximized and only weakly dependent on temperature, likely due to the fact that aggregates of only two to four proteins are predicted to be involved in freezing at -9°C (Govindarajan and Lindow, 1988) and single proteins of these bacteria are likely sufficient at somewhat colder temperatures. Thus, biases should be solely due to uncertainty in derived INP concentration in this colder temperature regime. The excellent agreement between all online and offline methods suggests biases of at most a factor of 5 in this case.

All immersion freezing methods (all results, including those for the IS, are from shared impinger samples in this case) capture the strong rise in activation due to the presence of the most active biological ice nucleators, within the realm of the Groups I and II defined by Yankofsky et al. (1981), noted as a pronounced shoulder in all freezing spectra at temperatures warmer than -8°C in Fig. 7. This has also been demonstrated by Wex et al. (2015), Budke and Koop (2015), and Polen et al. (2016). Nevertheless, discrepancies are most strongly apparent in this region where these larger and more fragile aggregates of ice nucleating proteins are responsible for the ice nucleation activity. Measurement discrepancies across all immersion freezing methods are seen to range from one to four orders of magnitude (up to 4°C equivalent difference), increasing toward the warmest temperatures in this temperature region in Fig. 7. This appears to result largely from a bifurcation of freezing behavior of the (warmest) first-freezers in multiple freezing scans of the thawed CMU-CS impinger sample, and a similarly strong increase in the activation of first freezers in a few NIPI scans that were processed without prior storage as a frozen sample (i.e., processed immediately after collection, the only group to do so), including following dilution of the sample performed in order to access colder freezing temperatures for droplet arrays. The CMU results in two of four scans appear to reflect the instability of Group I freezers noted in previous studies, possibly dependent on the time delay involved in conducting a freezing experiment following thawing of the impinger sample (Polen et al., 2016). How the individual freezing assays were separated for averaging is described in the Supporting Information. In summary, the source of variations in activity seen in the warmest activation temperature regime for Snomax® particles question the ability to utilize the warmest temperature (> -10°C) freezing behavior of Snomax® reliably for calibration purposes, as similarly noted by Polen et al. (2016) (e.g., due to batch variability and loss of activity in storage). The freezing behaviors at colder than -10°C are quite stable, and a simple conclusion from this experiment is that there is no fundamental limitation or apparent bias in the ability of any method (online or offline) to measure immersion freezing activation in the modestly



supercooled temperature regime warmer than -15°C versus below -20°C, at least for detecting biological INPs in relatively high numbers. Hence, if disagreements occur between online and offline methods in this temperature regime, one possibility is that such disagreement relates to the impact of immersion in water on ice nucleation activity for certain particle types whose morphology can be altered in water (e.g., Grawe et al., 2016) and/or other differences in activation of single particles by online methods versus particle populations placed into bulk water, sometimes stored frozen for later processing.

### 3.2 Sampling of INPs from the AIDA chamber and comparison to subsequent AIDA freezing results

Data collected in coordination with AIDA experiments provided additional intercomparisons. These data were first analyzed as active fractions, which is the number fraction of all particles freezing when normalized to the number concentrations of single INP types present at the onset of expansions. Because of the large volume of the AIDA chamber, only modest differences in aerosol particle concentrations existed in the time prior to expansion start. Despite more limited participation, most online measurement systems and a few offline diffusion chamber systems processed particles in these experiments. Generally lower INP number concentrations in AIDA limited any chance that INP number concentrations achieve values that might lead to vapor depletion in the continuous flow instruments (Levin et al., 2016). Use of active fraction allowed for inclusion and comparison of data from multiple AIDA experiments, and from APC experiments, to examine for consistency and repeatability. As discussed in Section 2.4, the active fraction data could be readily converted to active site density.

In Fig. 8, results are included for the illite NX, for which comprehensive experiments in the APC were not examined in Section 3.1. Figure 8a shows active fraction data from various ice nucleation instruments in multiple AIDA experiments (listed in Fig. 8 caption and Table S1), and from the ice concentrations measured in subsequent AIDA expansions. These results for illite NX show a scatter of INP active fraction at selected temperatures of more than two orders of magnitude, consistent with Hiranuma et al. (2015). Data from two FRIDGE-STD wafer collections demonstrate a variability factor of several fold despite collection of the particles in close temporal proximity. This could reflect the negative impacts of excess particle loading on causing water vapor depletion in the diffusion chamber as freezing ensues, limiting full activation at 1% supersaturation. Consistent with such an assumption, we note that sample 73 (lower set of FRIDGE-STD data points at -25 and -30°C) had four times the volume of sample 74 (higher active fraction data points at -25 and -30°C). The convergence of the FRIDGE-STD results toward the FRIDGE-IMM results is also noted for the latter sample. This issue of determining the suitable volume of air for collection for substrate ice nucleation studies given its dependence on the concentration of INPs has been recognized for many years. Nevertheless, correspondingly low active fractions at -25°C are also measured by PINC, a flow diffusion chamber that should have no issues with water vapor depletion. We may note, however, the strong sensitivity to processing supersaturation in flow diffusion chambers for sampling illite NX particles as reflected by the CFDC-CSU results at 105% and maximum $RH_w$ prior to onset of water droplet breakthrough. We may further note that AIDA activated ice number fractions for illite NX are bracketed by these CFDC-CSU results. These results are consistent with the findings of DeMott et al. (2015) for certain natural and desert dusts, suggesting that underestimates of INP concentrations active in the water supersaturated regime where immersion freezing sometimes dominates in CFDCs could be a

Atmos. Meas. Tech. Discuss., https://doi.org/10.5194/amt-2018-191
Manuscript under review for journal Atmos. Meas. Tech.
Discussion started: 10 July 2018




general feature, also discussed by Garimella et al. (2017). A strong sensitivity of illite NX to $RH_w$ may be partly responsible for the wider range of INP active fraction for diffusion chambers in this case, and the shorter residence time of the PINC instrument may contribute to its lower estimate in comparison to other continuous flow chambers at certain temperatures. Each continuous flow chamber also may stimulate different responses in regard to $RH_w$ sensitivity, dependent on a variety of factors in addition to residence time that may include the evaporation section control. These things may require special study for the flow diffusion chambers as a group.

Data are plotted as $n_{s,geo}$ *(T)* values in Fig. 8b, and parameterizations developed from the study by Hiranuma et al. (2015) are overlain. This demonstrates that the single DFPC-ISAC chamber data point at -20°C and the upper bound values of FRIDGE-STD measurements are consistent with the $n_{s,geo}$ curve (log-space version shown as long-dashed curve) function found to represent immersion freezing measurement data by Hiranuma et al. (2015). A fair amount of the online instrument data from AIDA sampling is also consistent with this function. Nevertheless, it is also the case that some portion of the online instrument data, particularly the CIC, CFDC-CSU measurements at maximum water supersaturation, AIDA expansion results, and all lower temperature flow diffusion chamber data including the PIMCA-PINC, generally align with the Hiranuma et al. (2015) parameterization for results obtained from dry dispersion measurements in that study (short-dashed line in Fig. 8b). The FRIDGE-IMM results at warmer temperatures appear as the outlier, splitting the two parameterizations at the warm end of measurements.

When $n_{s,geo}$ *(T)* values derived from APC experimental results on illite NX particles are added in Fig. 8c, it becomes clear that most offline immersion freezing results in the present study align quite well with the parameterization of offline immersion freezing results from Hiranuma et al. (2015). Furthermore, it is seen that the DFPC-ISAC and FRIDGE-STD results, and the lower range of CFDC-type measurements (PINC, CFDC-TAMU) are most consistent with the immersion freezing data. However, we note the addition in Fig. 8c of CFDC-type measurements from APC experiments, including data from the CFDC-CSU, INKA, and SPIN-TROPOS instruments, which trend toward the dry suspension parameterization from Hiranuma et al. (2015). Most strikingly, these data, while limited to a few additional experiments, support the extension of this dry suspension relation to temperatures near -20°C, with the consequence that a three-order magnitude or more discrepancy occurs between online and offline measurements at this temperature. The data noted in blue for CFDC-CSU and INKA were the only data collected in the March 13 experiment. Nothing peculiar stands out for the aerosol generated on that day, with sizes that did not reach close to ice crystal detection sizes. Hence, the bifurcation of INP behaviors of illite NX at different times and potentially by different methods are confirmed in the present study, and with no special new insights as yet into their source nor of the relevance of these discrepancies as a potential concern for atmospheric INP measurements. While proposed as an atmospheric dust surrogate, the ice nucleation behaviors of illite NX assessed by different methods contrast with the general equivalency of measurements of INP behaviors of natural soil dusts found in this study.

Agreement of methods for measuring the INP activity of Snomax® particles as shown in Fig. 7 is repeated in the AIDA experiments, as shown by $n_{s,geo}$ *(T)* calculations presented in Fig. 9a. Ice active site densities derived from fractional activation and particle surface areas in the AIDA experiments (listed in Fig. 9 caption) fall to the high side of other online measurements, but only by a modest factor of no more than a few, and within experimental uncertainties. Little difference is seen between CFDC-CSU results at 105% or the maximum $RH_w$ achieved before

Atmos. Meas. Tech. Discuss., https://doi.org/10.5194/amt-2018-191
Manuscript under review for journal Atmos. Meas. Tech.
Discussion started: 10 July 2018




water droplet breakthrough. As well, there is no discrepancy seen between the FRIDGE-STD and other results. This may be because Snomax® INPs have been observed to achieve their maximum activated fraction by 100% $RH_w$ at temperatures below -10°C (DeMott et al., 2011), and so no strong artificial supersaturation dependence occurs. Prediction of $n_{s,geo}$ *(T)* on the basis of the $n_m$ *(T)* (active site density per unit mass) determined in the Snomax® particle ice nucleation studies of Wex et al. (2015) is also presented in Fig. 9a. This conversion uses $n_m$ *(T)* as given in Eq. 6 of Wex et al. (2015), divided by the surface area to mass concentration ratio, following Eq. 3 from Hiranuma et al. (2015). A surface area to mass concentration ratio value of 7.99 $m^2$ $g^{-1}$ was derived from the Snomax® particle size distribution measurements made in association with the AIDA results reported in Wex et al. (2015). Particle generation methods for Snomax® used in the present AIDA experiments were identical to that prior study. It is seen that although the peak predicted $n_{s,geo}$ *(T)* values exceed the values measured by most methods in this study, it is by only a small amount. Since this demonstrates close consistency of the present experiments with past Snomax® experiments, we did not pursue the exercise of re-deriving the surface to mass concentration ratio particular to the FIN-02 studies. APC data were used to derive $n_{s,geo}$ *(T)* in Fig. 9b. This demonstrates repeatability during the FIN-02 studies for assessment of the ice nucleation activity of Snomax® INPs and a level of consistency with prior results that suggests the potential suitability of Snomax® as a bacterial INP calibrant surrogate, albeit with the mentioned caveats on the instability of detection of first freezers at the warmest temperatures.

AIDA experimental results converted to $n_{s,geo}$ *(T)* for Argentinian and Tunisian soil dusts are shown in Fig. 10a. As expected, the range of site density measured by the continuous flow chambers prior to expansion, and based on AIDA ice activation measurements during expansion, mimics a similar spread in INP number concentrations observed by all measuring systems in sampling from the APC. We also note the agreement between AIDA ice crystal activation in cloud parcel simulations and the INP measurements from the portable instruments in these two cases at near -25°C. The non-continuous-flow diffusion chamber results from these AIDA chamber experiments fall moderately to the low side of $n_{s,geo}$ *(T)* values for these dusts. The two dusts have similar activation properties at below -20°C, and the range of $n_{s,geo}$ *(T)* is at least partly consistent with multiple natural soil dust $n_{s,geo}$ *(T)* parameterizations, including O'Sullivan et al. (2014) for "fertile soil dust", Tobo et al. (2014) for "Wyoming soil dust" and Steinke et al. (2016) for "agricultural soil dust". Derived $n_{s,geo}$ *(T)* based on the APC experiments on Argentinian dust (Fig. 4) are overlain in panel b, and $n_{s,geo}$ *(T)* derived from APC Tunisian dust experimental data (Fig. 5) is overlain in panel c of Fig. 10. In contrast to larger discrepancies found for illite NX, $n_{s,geo}$ *(T)* results for both Argentinian and Tunisian dust shown in Fig. 10 demonstrate much greater consistency. Larger discrepancies occur only at the coldest temperatures, where the PIMCA-PINC measurements of direct freezing of single particles within droplets diverge to much higher values than most of the immersion freezing measurements. This is especially the case for the Tunisian dust results, where $n_{s,geo}$ *(T)* based on the maximum $RH_w$ INP data from the CFDC-CSU do not clearly align with the PIMCA-PINC results in the same manner that they do for Argentinian dust at colder temperatures. The WISDOM data also diverge strongly from other immersion freezing data at colder than -25°C. Finally, we may note that the $n_{s,geo}$ *(T)* results for the more loamy Argentinian dust align quite well with values predicted from previous studies of arable soil dusts in the studies of O'Sullivan et al. (2014) and Tobo et al. (2014), but not well with those predicted from Steinke et al. (2016). The

Atmos. Meas. Tech. Discuss., https://doi.org/10.5194/amt-2018-191
Manuscript under review for journal Atmos. Meas. Tech.
Discussion started: 10 July 2018




Tunisian dust results in Fig. 10c show less consistency with the fertile soil dust parameterization, which may be expected due to the more arid nature of the Tunisian sample.

Finally, $n_{s,geo}$ *(T)* results for sampling K-feldspar particles from AIDA prior to expansions are shown in Fig. 11a, and the same data are overlain with APC data for K-feldspar in Fig. 11b. Additionally, an $n_{s,geo}$ *(T)* parameterization is added on the basis of the $n_{s,BET}$ *(T)* fit to immersion freezing ice nucleation data published by Atkinson et al. (2013), where the BET refers to the fact that the surface area employed is based on Brunauer–Emmett–Teller (BET) gas adsorption data rather than an estimate of geometric surface area. To convert the parameterization, we use the laser diffraction-based surface-to-mass conversion factor of 0.89 $m^2$ $g^{-1}$ determined by Atkinson et al. (2013) and the specific BET surface area measured for the samples used in this study of 2.6 $m^2$ $g^{-1}$. Hence, the normalization factor is 2.6/0.89. While all of the data parallel the Atkinson et al. (2013) parameterization, agreement with it quantitatively is seen for selected online instrument data and the limited AIDA data available for which water saturation was achieved in expansion tests for FS02. Exceptionally large spread in inferred $n_{s,geo}$ values occurs at -20°C. Note here that only the 105% $RH_w$ data was usable for the CFDC-CSU and INKA instruments in this case because of an issue that was associated with and exacerbated by the steep activation curve of K-feldspar at this temperature. In particular, it was seen that very steep $n_{s,geo}$ *(T)* led to the appearance of small ice crystals in the optical particle counter spectra at just above the 3 μm size used to separate smaller liquid from larger ice particles. This is an unusual feature for this type of device, with nucleated ice crystals typically growing to larger optical channels (sizes), and it likely reflects the late freezing of liquid particles as they were evaporating and cooling upon entry into the evaporation region of the instruments. This possibility is unique to the present configuration of the CSU CFDC design due to the adjustment of the walls in evaporation region to match the inner (cold) wall temperature. This issue could similarly be realized in any diffusion chamber if there is a "cold point" anywhere along the flow path. Consequently, the SPIN-MIT data shown were reprocessed to report their data at the coldest wall temperature measured in the instrument growth region. Further discussion of this issue is provided for the CFDC-CSU in the Supplement to this paper (Section S.1.2). An additional (red) data point is shown in Fig. 11 for the CFDC that is considered erroneously attributed to the activation temperature near -20°C, even though it aligns close to the AIDA chamber data. In this case, it was found that the rate of $RH_w$ change during scanning from lower to higher values was too fast, and exacerbated the over-estimation of INPs on the basis of OPC particle size. We note that the INKA instrument used a larger channel (size) to count INPs, and at the reported water supersaturation 4%, smaller the ice crystals were not being counted. Hence, the ice size channel might have been redefined for the CSU instrument in order to report additional data, but we choose here to use the data instead to make a point about instrument design considerations. As a final note, it should be understood that scans of $RH_w$ are not a typical operational practice when collecting atmospheric data. In this case, constant $RH_w$ or step-wise values are used.

While the various $n_{s,geo}$ *(T)* data trend well overall with the previous parameterization for FS02 particles, correspondence amongst results in Fig. 11 is not as good as for the soil dust samples in the -20 to -25°C range, and more resemble the spread of results for illite NX, with separation of $n_{s,geo}$ *(T)* of up to three orders of magnitude. Again, the variance amongst measurements follows the steepness of the INP activity versus temperature. The steep ice activation function of K-feldspar in the region from -15 to -25°C has already been noted in Fig. 6. INP activity rises



at least $10^6$ times over the 10°C for K-feldspar in this range, whereas the steepest rise for the natural soil dusts is $10^3$ to $10^4$ units per 10°C. For illite NX the activity rises about $10^5$ per 10°C. Thus, modest differences in temperature, or their control within instruments, equate to large differences in ice activation for K-feldspar.

**4 Summary and Conclusions**

Through careful coordination and collaboration in a laboratory setting, most of the objectives of the second phase of the Fifth Ice Nucleation Workshop were advanced if not fully achieved, and the existence of the data set should continue to serve explorations of measurement consistencies and issues for applying different techniques in isolation or in tandem for making atmospheric ice nucleation measurements. We particularly note that some data were not added to this paper in circumstances where a clear error or measurement bias was occurring based on the experience of the instrument team. Some of these were investigated, as noted in the manuscript above. Others remain the subject of active investigation.

To simplify this first analysis of FIN-02 data, a focus was placed in this paper on immersion freezing nucleation and activation within continuous flow chambers in the water supersaturated regime, across a wide temperature range including temperatures warmer than -15°C through the use of bacterial INPs in selected experiments. Excellent correspondence was obtained between many measurements for soil dusts and bacterial INPs across online and offline methods (Figures 4 – 7). Agreement of geometric active site density within less than about 1 order of magnitude was achieved under most circumstances analyzed herein for these three materials. For the atmospherically-relevant particle types examined, no strong biases between online and offline measurement systems were evident in their range of overlap except primarily in the case of illite NX, where discrepancies seen in Hiranuma et al. (2015) were reproduced at temperatures warmer than -25°C. The fact that agreements were much better overall in this study may be due to co-sampling the same aerosol particle sources in the same laboratory, sharing similar collected aerosol samples, and limiting the largest particle sizes assessed in workshop experiments to those that could readily be measured by all techniques. The nature of active sites for the various INPs examined may also have influenced comparability of online and offline methods across the mixed-phase cloud temperature regime. Consequently, it appears that soil dust particles are much more equally assessed for INP content than some minerals and mineral mixtures. This was supported by the worst agreement between methods, up to three orders of magnitude, for illite NX and the FS02 samples that have a very steep activation spectra versus temperature, which exacerbates disagreements that otherwise represent only a few degrees of temperature change. Productively, this behavior of the FS02 led to new discovery of instrument behavior in the case of the CFDC instruments. It is worth noting that most natural INP T-spectral slopes are lower than for many of the samples tested, often only approximately 2 orders of magnitude per 10°C, rather than 5 orders or more per 10°C (DeMott et al., 2017; Price et al., 2018).

Assessment of agreement between online and offline measurement systems is mostly only possible below -20°C since online devices have a limit of detection which restricts measurements at warmer temperatures. The exception is in cases where the higher concentrations of bacterial INPs were assessed. Since biological/biogenic INPs are the most likely contributors to freezing at modest supercooling (e.g., Murray et al., 2012; Hoose and Möhler, 2012), it would seem valid that combining offline measurements to capture INPs at very modest supercooling with online



measurements extending to colder temperatures within the same atmospheric study will lead to a valid representation of immersion freezing INPs (e.g., DeMott et al., 2017; Welti et al., 2018).

Among offline measurements, there appears no particular or consistent bias between different approaches to bulk suspension measurements. Furthermore, there appears to be little discrepancy between measurements made with particles collected directly into liquid versus collection onto filters followed by resuspension into liquid. There also appear to be no discernable impacts of freezing samples versus processing them immediately, on the basis of the µl-NIPI versus other methods apart from impacts on the warmest temperature freezing of bacterial particles (e.g., results from Snomax® experiments). Factors affecting reproducibility, such as accuracy of temperature attributed to sample freezing and instability of the warmest bacterial INPs, are the most important factors affecting the agreement between methods, which often spans an order of magnitude overall. Most offline measurement groups have likely performed careful assessments of their temperature measurements attributed to droplet volumes, but there is evidence that errors may occur due to the inability to perfectly assess temperature at the point of freezing (Beall et al., 2017).

For offline diffusion chamber measurements of collected particles, the need for awareness of volume effects on processed INPs remains as a requirement. Results in a few cases showed these measurements to fall to the low side in assessing immersion freezing nucleation. It may be necessary to collect varied volumes to assure that particle loading in different cases is not influencing accurate assessment of INP number concentrations.

Of note in this study is the agreement between most online and offline measurements at the colder temperatures in comparison to the large discrepancies found in a recent study comparing measurements of ambient particles (DeMott et al., 2017). We believe that this is attributable to assuring comparability of measurement methods in FIN-02 by restricting particle sizes so that all methods capture most of the largest particles in the distribution. This likewise implies that discrepancies can be expected to occur in ambient sampling when larger particles are present, although the source of those discrepancies as true impacts (i.e., of larger particles acting as individual INPs versus de-agglomeration of INPs after time in bulk suspensions) must remain a topic of research. Both offline immersion freezing and proximal freezing in the online diffusion chambers sometimes underestimates freezing in comparison to the PIMCA-PINC single particle immersion freezing method. For CFDC type instruments, this is understood as the need to achieve much higher $RH_w$, sometimes practically unachievable, to effectively simulate and capture immersion freezing, requiring corrections not applied in this study. Reasons why the offline immersion freezing methods do not always agree with PIMCA-PINC may relate in some unresolved manner to the full immersion of all particles into the same liquid volume. It would be helpful if the PIMCA-PINC method could be extended to lower active fractions and INP concentrations, but this appears to be a fundamental limitation of the phase discrimination technique.

Differences between INP measurements in the water-supersaturated regime by online continuous flow chambers were seen, and again these differences likely relate to the artificial need of these systems to achieve higher than expected $RH_w$ in order to fully activate aerosols to facilitate their subsequent immersion freezing on the full particle population within the diffusion chambers (DeMott et al., 2015; Garimella et al., 2017; Burkert-Kohn et al., 2017). These instruments may universally have an issue in focusing aerosol particles reliably into the center of the imposed $RH_w$ field, among other factors that depend on particle types, including their hygroscopicity and ability to activate ice nucleation already in the sub-water saturated regime (not discussed in this paper). Solving the issue(s) involved could



provide the decision on correcting these data for the $RH_w$-sensitivity factor present in the water supersaturated regime for all of these devices. Different systems have varied ability to achieve higher $RH_w$, depending on the different water breakthrough $RH_w$ as imposed by device design (see Section 3 and Section S.1.2). These systems will continue to be used in this manner to measure atmospheric INP activation, but will struggle to uniformly capture activation to the same degree until issues are solved. This is clearly deserving of special study, which was beyond the scope of this workshop. Study of the use of different evaporation region temperatures also merits attention as it may impact detection of ice formation at higher $RH_w$. Limitations on assessing the impacts of larger aerosols as INPs in continuous flow instruments will remain, unless special inlets are developed.

Workshops such as FIN-02 will continue to play a large role in assessing measurement biases and ultimately improving the comparability of INP measurements made by a large community of researchers sampling on a global scale. The shared experience of these workshops is irreplaceable in providing special insights into the status of and issues involved in obtaining INP data in different scenarios that may be dominated by certain aerosol types. As recommendations for the future of such studies, the FIN-02 campaign suggests continued efforts to co-sample the same aerosol systems or perform analysis on common samples. Special attention to co-sampling the temperature regime warmer than -20°C should be made, since only certain INP particle types presently allow comparison for both online and offline systems. This may entail design/use of aerosol particle concentrating systems to facilitate such comparisons. Experiments alternately including or excluding super-micrometer particles would allow specific inspection of biases that can occur, especially between online and offline measurement systems for certain aerosol systems. Further studies on the bases of the need for continuous flow chambers to achieve higher water supersaturations to fully activate ice formation, and for what circumstances and aerosol particle types, would also be useful. Comparisons for which the sampling groups are "blind" to the nature and concentrations of INPs being sampled could be useful toward giving confidence to the wider community that the INP measurement community is capable of recognizing issues and properly interpreting data. This will assist confidence and utility of larger global data sets. Such a comparison from FIN-02 will be reported on in a separate publication in preparation. Similar exercises as FIN-02 are also needed in sampling under ambient atmospheric conditions. This is the subject of the FIN-03 campaign that will be reported on separately.

Finally, the FIN-02 archive will remain for additional scientific investigations, such as comparisons in the ice nucleation regime below water saturation, analysis of experiments regarding homogeneous freezing and the role of particle pre-activation for ice formation. FIN-02 demonstrates that the INP measurement community remains on a progressive track towards convergence between different methods used for INP quantification.

*Data availability.* Tables of all data used and plotted in this manuscript are included as Table S1 and Table S2 in the Supplement of this manuscript. These tables are also included with data archived in the KITopen data respository under doi:10.5445/IR/1000082906 (available upon publication). Other data are available upon request.

*Competing interests.* The authors declare no competing interests.



*Special issue statement.* This article is part of the special issue "Fifth International Workshop on Ice Nucleation (FIN)". It is not associated with a conference.

*Acknowledgments.* The FIN-02 campaign was partially-supported by U.S. National Science Foundation Grant # AGS-1339264, and by the U.S. Department of Energy's Atmospheric System Research, an Office of Science, Office of Biological and Environmental Research program, under Grant No. DE-SC0014487. P. J. DeMott, E. J. T. Levin, and K. J. Suski acknowledge additional support from NSF Grant # AGS-1358495. The following authors acknowledge funding by the German Science Foundation (DFG) through the research unit FOR 1525 (INUIT): O. Möhler, N. Hiranuma, A. Peckhaus and A. Kiselev under MO 668/4-1, C. Budke and T. Koop under KO 2944/2-2, M. Szakáll and O. Eppers under SZ260/4-2, and H. Bingemer and D. Weber under BI 462/3-2. Y. Rudich acknowledges funding by the DFG Mercator fellowship. T.B. Kristensen acknowledges funding from the German Federal Ministry of Education and Research (BMBF) project 01LK1222B. A. Welti, P. Herenz, F. Belosi, G. Santachiara, J. Vergara-Temprado, H. Bingemer and J. Schrod acknowledge support funding for their research from the European Union's Seventh Framework Programme (FP7/2007-2013) project BACCHUS under grant agreement No. 603445. F. Belosi and G. Santachiara also acknowledge the Institute for Atmospheric and Environmental Sciences (Goethe-University Frankfurt) for support in filter collections. M. Burkert-Kohn was funded by grant no. ETH-17 12-1, ETH Zurich. H. Grothe, L. Felgitsch, and T. Seifried acknowledge funding from The Austrian Science Fund, FWF project number P26040. The University of Leeds team (T. F. Whale, H. P. Price, J. Vergara-Temprado, D. O'Sullivan, T. W. Wilson, and B. J. Murray) acknowledge support from the European Research Council (ERC, 240449 ICE; 632272 IceControl; 648661 MarineIce, 713664 CryoProtect) and the Natural Environment Research Council (NE/K004417/1, NE/I019057/1). S. D. Brooks, K. N. Collier, and J. Zenker acknowledge additional support from the U.S. National Science Foundation, Grant # ECS-1309854. M. J. Polen and R. C. Sullivan were supported by NSF Grants # CHE-1213718 and CHE-1554941, and M. J. Polen by an NSF Graduate Research Fellowship. M. D. Petters, S. S. Petters, and H. P. Taylor acknowledge additional support from NSF Grants # AGS-1010851 and # AGS-1450690. G. Kulkarni acknowledges support by the Office of Science of the U.S. Department of Energy (DOE) as part of the Atmospheric System Research Program. Pacific Northwest National Laboratory is operated for the U.S. DOE by Battelle Memorial Institute under contract DEAC05-76RL0 1830. Finally, all authors wish to acknowledge support from the AIDA team for preparing and operating the AIDA chamber, and supporting other operational logistics for this workshop.

**References**

Agresti, A. and Coull, B. A.: Approximate is better than "exact" for interval estimation of binomial proportions, The American Statistician, 52, 119-126, doi:10.1080/00031305.1998.10480550, 1998.

Archuleta, C. M., DeMott, P. J., and Kreidenweis, S. M.: Ice nucleation by surrogates for atmospheric mineral dust and mineral dust/sulfate particles at cirrus temperatures, Atmos. Chem. Phys., 5, 2617–2634, doi:10.5194/acp-5-2617-2005, 2005.



Ardon-Dryer, K. and Levin, Z.: Ground-based measurements of immersion freezing in the eastern Mediterranean, Atmos. Chem. Phys., 14, 5217-5231, doi:10.5194/acp-14-5217-2014, 2014.

Atkinson, J. D., Murray, B. J., Woodhouse, M. T., Whale, T. F., Baustian, K. J., Carslaw, K. S., Dobbie, S., O'Sullivan, D., and Malkin, T. L.: The importance of feldspar for ice nucleation by mineral dust inmixed-phase clouds, Nature, 498, 355-358, doi:10.1038/nature12278, 2013.

Baron, P. A., and Willeke, K., *Aerosol Measurement: Principles, Techniques, and Applications*, Second Edition, Wiley, 2005.

Beall, C. M., Stokes, M. D., Hill, T. C., DeMott, P. J., DeWald, J. T., and Prather, K. A., 2017: Automation and Heat Transfer Characterization of Immersion Mode Spectroscopy for Analysis of Ice Nucleating Particles, Atmos. Meas. Tech., 10, 2613-2626, https://doi.org/10.5194/amt-10-2613-2017.

Belosi, F., Santachiara, G., and Prodi, F.: Ice-forming nuclei in Antarctica: New and past measurements, Atmospheric Research 145–146, 105–11, doi:10.1016/j.atmosres.2014.03.030, 2014.

Benz, S., Megahed, K., Möhler, O., Saathoff, H., Wagner, R., and Schurath, U.: T-dependent rate measurements of homogeneous ice nucleation in cloud droplets using a large atmospheric simulation chamber, J. Photochem. Photobiol. A, 176, 208–217, doi:10.1016/j.jphotochem.2005.08.026, 2005.

Beydoun, H., Polen, M., and Sullivan, R. C.: Effect of particle surface area on ice active site densities retrieved from droplet freezing spectra. Atmos. Chem. Phys., 16, 13359–13378, doi:10.5194/acp-16-13359-2016, 2016.

Beydoun, H., Polen, M. and Sullivan, R. C.: A new multicomponent heterogeneous ice nucleation model and its application to Snomax bacterial particles and a Snomax–illite mineral particle mixture, Atmos. Chem. Phys., 17(22), 13545–13557, doi:10.5194/acp-17-13545-2017, 2017.

Boose, Y., Kanji, Z. A., Kohn, M., Sierau, B., Zipori, A., Crawford, I., Lloyd, G., Bukowiecki, N, Herrmann, E., Kupiszewski, P., Steinbacher, M. and U. Lohmann: Ice Nucleating Particle Measurements at 241K during Winter Months at 3580m MSL in the Swiss Alps, J. Atmos. Sci., 73, 2203-2228, 2016.

Buck, A.L.: New equations for computing vapour pressure and enhancement factor. J. Appl. Meteorol., 20, 1527–1532, doi:10.1175/1520-0450(1981)020<1527:NEFCVP>2.0.CO;2, 1981.

Budke, C. and Koop, T.: BINARY: an optical freezing array for assessing temperature and time dependence of heterogeneous ice nucleation, Atmos. Meas. Tech., 8, 689–703, doi:10.5194/amt-8-689-2015, 2015.

Burkert-Kohn, M., Wex, H., Welti, A., Hartmann, S., Grawe, S., Hellner, L., Herenz, P., Atkinson, J D., Stratmann, F., and Kanji, Z. A.: Leipzig Ice Nucleation chamber Comparison (LINC): intercomparison of four online ice nucleation counters. Atmos. Chem. Phys., 17, 11683–11705, https://doi.org/10.5194/acp-17-11683-2017, 2017.

Chou, C., Stetzer, O., Weingartner, E., Juranyi, Z., Kanji, Z. A. and Lohmann, U.: Ice nuclei properties within a Saharan dust event at the Jungfraujoch in the Swiss Alps, Atmos. Chem. Phys., 11(10), 4725-4738, doi:10.5194/acp-11-4725-2011, 2011.

Delort, A.-M., and Amato, P., Eds., *Microbiology of Aerosols*, John Wiley & Sons, Inc., 1st Edition, ISBN: 978-1119132288, 2018.

DeMott, P. J., Möhler, O., Stetzer, O., Vali, G., Levin, Z., Petters, M. D., Murakami, M., Leisner, T., Bundke, U., Klein, H., Kanji, Z., Cotton, R., Jones, H., Petters, M., Prenni, A., Benz, S., Brinkmann, M., Rzesanke, D.,



Saathoff, H., Nicolet, M., Gallavardin, S., Saito, A., Nillius, B., Bingemer, H., Abbatt, J., Ardon, K., Ganor, E., Georgakopoulos, D. G., and Saunders, C.: Resurgence in ice nucleation research. Bull. Amer. Meteor. Soc., 92, 1623-1635, doi:10.1175/2011BAMS3119.12011, 2011.

DeMott, P. J., Prenni, A. J., McMeeking, G. R., Tobo, Y., Sullivan, R. C. , Petters, M. D., Niemand, M., Möhler, O., and Kreidenweis, S. M.: Integrating laboratory and field data to quantify the immersion freezing ice nucleation activity of mineral dust particles, Atmos. Chem. Phys., 15, 393–409, doi:10.5194/acp-15-393-2015, 2015.

DeMott, P. J., Hill, T. C. J., Petters, M. D., Bertram, A. K., Tobo, Y., Mason, R, H., Suski, K. J., McCluskey, C. S., Levin, E. J. T., Schill1, G. P., Boose, Y., Rauker, A. M., Miller, A. J., Zaragoza, J., Rocci, K., Rothfuss, N. E., Taylor, H. P., Hader, J. D., Chou, C., Huffman, J. A., Pöschl, U., Prenni, A. J., and Kreidenweis, S. M.: Comparative measurements of ambient atmospheric concentrations of ice nucleating particles using multiple immersion freezing methods and a continuous flow diffusion chamber, Atmos. Chem. Phys., 17, 11227–11245, 2017.

Di Biagio, C., Formenti, P., Styler, S. A., Pangui, E. and Doussin, J.-F.: Laboratory chamber measurements of the longwave extinction spectra and complex refractive indices of African and Asian mineral dusts, Geophys. Res. Lett., 41, 6289–6297, doi:10.1002/2014GL060213, 2014.

Diehl, K., Debertshäuser, M., Eppers, O., Schmithüsen, H., Mitra, S. K., and Borrmann, S.: Particle surface area dependence of mineral dust in immersion freezing mode: investigations with freely suspended drops in an acoustic levitator and a vertical wind tunnel, Atmos. Chem. Phys., 14, 12343-12355, doi:10.5194/acp-14-12343-2014, 2014.

Eidhammer, T., DeMott, P. J., Prenni, A. J., Petters, M. D., Twohy, C. H., Rogers, D. C., Stith, J., Heymsfield, A., Wang, Z., Haimov, S., French, J., Pratt, K., Prather, K., Murphy, S., Seinfeld, J., Subramanian, R., and Kreidenweis, S. M.: Ice initiation by aerosol particles: Measured and predicted ice nuclei concentrations versus measured ice crystal concentrations in an orographic wave cloud, J. Atmos. Sci., 67, 2417–2436, doi:10.1175/2010JAS3266.1, 2010.

Emersic, C., Connolly, P. J., Boult, S., Campana, M., and Li, Z.: Investigating the discrepancy between wet-suspension- and dry dispersion-derived ice nucleation efficiency of mineral particles, Atmos. Chem. Phys., 15, 11311–11326, doi:10.5194/acp-15-11311-2015, 2015.

Fahey, D. W., Gao, R.-S., Möhler, O., Saathoff, H., Schiller, C., Ebert, V., Krämer, M., Peter, T., Amarouche, N., Avallone, L. M., Bauer, R., Bozóki, Z., Christensen, L. E., Davis, S. M., Durry, G., Dyroff, C., Herman, R. L., Hunsmann, S., Khaykin, S. M., Mackrodt, P., Meyer, J., Smith, J. B., Spelten, N., Troy, R. F., Vömel, H., Wagner, S., and Wienhold, F. G.: The AquaVIT-1 intercomparison of atmospheric water vapor measurement techniques, Atmos. Meas. Tech., 7, 3177-3213, doi:10.5194/amt-7-3177-2014, 2014.

Fan, J., Leung, L. R., Rosenfeld, D. and DeMott, P. J.: Effects of Cloud Condensation Nuclei and Ice Nucleating Particles on Precipitation Processes and Supercooled Liquid in Mixed-phase Orographic Clouds, Atmos. Chem. Phys., 17, 1017–1035, doi:10.5194/acp-17-1017-2017, 2017.



Friedman, B., Kulkarni, G., Beránek, J., A. Zelenyuk, A., Thornton, J. A., and D. J. Cziczo, D. J.: Ice nucleation and droplet formation by bare and coated soot particles, J. Geophys. Res., 116, D17203, doi:10.1029/2011JD015999, 2011.

Garimella, S., Kristensen, T. B., Ignatius, K., Welti, A., Voigtländer, J., Kulkarni, G. R., Sagan, F., Kok, G. L., Dorsey, J., Nichman, L., Rothenberg, D. A., Rösch, M., Kirchgäßner, A. C. R., Ladkin, R., Wex, H., Wilson, T. W., Ladino, L. A., Abbatt, J. P. D., Stetzer, O., Lohmann, U., Stratmann, F., and Cziczo, D. J.: The SPectrometer for Ice Nuclei (SPIN): an instrument to investigate ice nucleation, Atmos. Meas. Tech., 9, 2781-2795, doi:10.5194/amt-9-2781-2016, 2016.

Garimella, S., Rothenberg, D. A., Wolf, M. J., David, R. O., Kanji, Z. A., Wang, C., Rösch, M., and Cziczo1, D. J.: Uncertainty in counting ice nucleating particles with continuous diffusion flow chambers, Atmos. Chem. Phys. Discuss., doi:10.5194/acp-2016-1180, 2017.

Glen, A. and Brooks, S. D.: Single particle measurements of the optical properties of small ice crystals and heterogeneous ice nuclei, AS&T, 48:1, 1123-1132, doi:10.1080/02786826.2014.963023, 2014.

Grawe, S., Augustin-Bauditz, S., Hartmann, S., Hellner, L., Pettersson, J. B. C., Prager, A., Stratmann, F., and Wex, H.: The immersion freezing behavior of ash particles from wood and brown coal burning, Atmos. Chem. Phys., 16, 13911-13928, doi:10.5194/acp-16-13911-2016, 2016.

Govindarajan, A. G., and Lindow, S. E.: Size of bacterial icenucleation sites measured in situ by radiation inactivation analysis, Proc. Natl. Acad. Sci. U. S. A., 85(5), 1334–1338, 1988.

Hader, J. D., Wright, T. P., and Petters, M. D.: Contribution of pollen to atmospheric ice nuclei concentrations, Atmos. Chem. Phys., 14, 5433–5449, doi:10.5194/acp-14-5433-2014, 2014.

Harrison, A. D., Whale, T. F., Carpenter, M. A., Holden, M. A., Neve, L., O'Sullivan, D., Vergara Temprado, J. and Murray, B J.: Not all feldspars are equal: a survey of ice nucleating properties across the feldspar group of minerals, Atmos. Chem. Phys., 16, 10927–10940, doi:10.5194/acp-16-10927-2016, 2016.

Hill, T. C. J., Moffett, B. F., DeMott, P. J., Georgakopoulos, D. G., Stump, W. L., and Franc, G. D.: Measurement of ice nucleation-active bacteria on plants and in precipitation by quantitative PCR. Appl. Environ. Microbiol. 80(4):1256-1267, doi:10.1128/AEM.02967-13, 2014.

Hill, T. C. J., DeMott, P. J., Tobo, Y., Fröhlich-Nowoisky, J., Moffett, B. F., Franc, G. D., and Kreidenweis, S. M.: Sources of organic ice nucleating particles in soils, Atmos. Chem. Phys., 16, 7195–7211, doi:10.5194/acp-2016-1, 2016

Hiranuma, N., Paukert, M., Steinke, I., Zhang, K., Kulkarni, G., Hoose, C., Schnaiter, M., Saathoff, H., and Möhler, O.: A comprehensive parameterization of heterogeneous ice nucleation of dust surrogate: laboratory study with hematite particles and its application to atmospheric models, Atmos. Chem. Phys., 14, 13145–13158, doi:10.5194/acp-14-13145-2014, 2014a.

Hiranuma, N., Hoffmann, N., Kiselev, A., Dreyer, A., Zhang, K., Kulkarni, G., Koop, T., and Möhler, O.: Influence of surface morphology on the immersion mode ice nucleation efficiency of hematite particles, Atmos. Chem. Phys., 14, 2315–2324, doi:10.5194/acp-14-2315-2014, 2014b.



Hiranuma, N., Augustin-Bauditz, S., Bingemer, H., Budke, C., Curtius, J., Danielczok, A., Diehl, K., Dreischmeier, K., Ebert, M., Frank, F., Ho mann, N., Kandler, K., Kiselev, A., Koop, T., Leisner, T., Möhler, O., Nillius, B., Peckhaus, A., Rose, D., Weinbruch, S., Wex, H., Boose, Y., DeMott, P. J., Hader, J. D., Hill, T. C. J., Kanji, Z. A., Kulkarni, G., Levin, E. J. T., McCluskey, C. S., Murakami, M., Murray, B. J., Niedermeier, D., Petters, M. D., O'Sullivan, D., Saito, A., Schill, G. P., Tajiri, T., Tolbert, M. A., Welti, A., Whale, T. F., Wright, T. P., and Yamashita, K.: A comprehensive laboratory study on the immersion freezing behavior of illite NX particles: a comparison of 17 ice nucleation measurement techniques, Atmos. Chem. Phys., 15, 2489–2518, doi:10.5194/acp-15-2489-2015, 2015.

Hoose, C., and Möhler, O.: Heterogeneous ice nucleation on atmospheric aerosols: a review of results from laboratory experiments, Atmos. Chem. Phys., 12, 9817–9854, doi:10.5194/acp-12-9817-2012, 2012.

Kanji, Z. A., Welti, A., Chou, C., Stetzer, O., and Lohmann, U.: Laboratory studies of immersion and deposition mode ice nucleation of ozone aged mineral dust particles, Atmos. Chem. Phys., 13(17), 9097-9118, doi:10.5194/acp-13-9097-2013, 2013.

Klein, H., Haunold, W., Bundke, U., Nillius, B., Wetter, T., Schallenberg, S., Bingemer, H.: A new method for sampling of atmospheric ice nuclei with subsequent analysis in a static diffusion chamber, Atmospheric Research, 96, 218-224, doi:10.1016/j.atmosres.2009.08.002, 2010.

Kohn, M., Lohmann, U., Welti, A., and Kanji, Z. A.: Immersion mode ice nucleation measurements with the new Portable Immersion Mode Cooling chAmber (PIMCA), J. Geophys. Res. Atmos., 121, 4713–4733, doi:10.1002/2016JD024761, 2016.

Kulkarni, G., China, S., Liu, S, Nandasiri, M., Sharma, N., Wilson, J., Aiken, A. C., Chand, D., Laskin, A., Mazzoleni, C., Pekour, M., Shilling, J., Shutthanandan, V., Zelenyuk, A., and Zaveri, R. A.: Ice nucleation activity of diesel soot particles at cirrus relevant temperature conditions: Effects of hydration, secondary organics coating, soot morphology, and coagulation, Geophys. Res. Lett., 43, 3580–3588, doi:10.1002/2016GL068707, 2016.

Kulkarni, G., and co-authors: A new method for operating a continuous flow diffusion chamber to investigate temperature and time dependence in immersion freezing study, in preparation for Atmospheric Measurement Technology Discussion, 2018.

Lafon, S., Sokolik, I. N., Rajot, J. L., Caquineau, S. and Gaudichet, A.: Characterization of iron oxides in mineral dust aerosols: Implications for light absorption, J. Geophys. Res., 111, D21207, doi:10.1029/2005JD007016, 2006.

Langer, G. and Rogers, J.: An Experimental Study of the Detection of Ice Nuclei on Membrane Filters and Other Substrata, J. Appl. Meteor., 14, 560-570, doi:10.1175/1520-0450(1975)014<0560:AESOTD>2.0.CO;2, 1975

Levin, E. J. T., McMeeking, G. R., DeMott, P. J., McCluskey, C. S., Carrico, C. M., Nakao, S., Stockwell, C. E., Yokelson, R. J., and Kreidenweis, S. M. (2016), Ice-nucleating particle emissions from biomass combustion and the potential importance of soot aerosol, *J. Geophys. Res. Atmos.*, 121, doi:10.1002/2016JD024879.

Lüönd, F., Stetzer, O., Welti, A., and Lohmann, U.: Experimental study on the ice nucleation ability of size-selected kaolinite particles in the immersion mode, J. Geophys. Res.-Atmos., 115(D14201), DOI:10.1029/2009jd012959, 2010.



McFarquhar, G. M., Ghan, S., Verlinde, J., Korolev, A., Strapp, J. W., Schmid, B., Tomlinson, J. M., Wolde, M., Brooks, S. D., Cziczo, D., Dubey, M. K., Fan, J., Flynn, C., Gultepe, I., Hubbe, J., Gilles, M. K., Laskin, A., Lawson, P., Leaitch, W. R., Liu, P., Liu, X., Lubin, D., Mazzoleni, C., Macdonald, A.-M., Moffet, R. C., Morrison, H., Ovchinnikov, M., Shupe, M. D., Turner, D. D., Xie, S., Zelenyuk, A., Bae, K., Freer, M., and Glen, A.: Indirect and Semi-direct Aerosol Campaign, Bulletin of the American Meteorological Society, 92, 183-201, 10.1175/2010bams2935.1, 2011.

Möhler, O., Stetzer, O., Schaefers, S., Linke, C., Schnaiter, M., Tiede, R., Saathoff, H., Krämer, M., Mangold, A., Budz, P., Zink, P., Schreiner, J., Mauersberger, K., Haag, W., Kärcher, B., and Schurath, U.: Experimental investigation of homogeneous freezing of sulphuric acid particles in the aerosol chamber AIDA, Atmos. Chem. Phys., 3, 211–223, doi:10.5194/acp-3-211-2003, 2003.

Möhler, O., Büttner, S., Linke, C., Schnaiter, M., Saathoff, H., Stetzer, O., Wagner, R., Krämer, M., Mangold, A., Ebert, V., and Schurath, U.: Effect of sulphuric acid coating on heterogeneous ice nucleation by soot aerosol particles, J. Geophys. Res., 110, D11 210, doi:10.1029/2004JD005 169, 2005

Möhler, O., Field, P. R., Connolly, P., Benz, S., Saathoff, H., Schnaiter, M.,Wagner, R., Cotton, R., Krämer, M., Mangold, A., and Heymsfield, A. J.: Efficiency of the deposition mode ice nucleation on mineral dust particles, Atmos. Chem. Phys., 6, 3007–3021, doi:10.5194/acp-6-3007-2006, 2006.

Murray, B. J., O'Sullivan, D., Atkinson, J. D., and Webb, M. E.: Ice nucleation by particles immersed in supercooled cloud droplets, Chem. Soc. Rev., 41(19), 6519–6554, doi:10.1039/C2CS35200A, 2012.

Murphy, D. M. and Koop, T.: Review of the vapour pressures of ice and supercooled water for atmospheric applications, Q. J. Roy. Meteor. Soc., 131, 1539–1565, doi/10.1256/qj.04.942005.

Niedermeier, D., S. Augustin-Bauditz, S. Hartmann, H. Wex, K. Ignatius, and F. Stratmann (2015), Can we define an asymptotic value for the ice active surface site density for heterogeneous ice nucleation?, J. Geophys. Res. Atmos., 120, 5036–5046, doi:10.1002/2014JD022814.

Niemand, M., Möhler, O., Vogel, B., Vogel, H., Hoose, C., Connolly, P., Klein, H., Bingemer, H., DeMott, P., and Skrotzki, J.: A particle-surface-area-based parameterization of immersion freezing on desert dust particles, J. Atmos. Sci., 69, 3077–3092, doi:10.1175/Jas-D-11-0249.1, 2012.

O'Sullivan, D., Murray, B. J., Malkin, T. L., Whale, T. F., Umo, N. S., Atkinson, J. D., Price, H. C., Baustian, K. J., Browse, J., and Webb, M. E.: Ice nucleation by fertile soil dusts: relative importance of mineral and biogenic components, Atmos. Chem. Phys., 14, 1853-1867, 2014.

O′Sullivan, D., Murray, B. J., Ross, J. F., Whale, T. F., Price, H. C., Atkinson, J. D., Umo, N. S., and Webb, M. E.: The relevance of nanoscale biological fragments for ice nucleation in clouds, Sci. Rep., 5, 2015.

Peckhaus, A., Kiselev, A., Hiron, T., Ebert, M., and Leisner, T.: A comparative study of K-rich and Na/Ca-rich feldspar ice-nucleating particles in a nanoliter droplet freezing assay, Atmos. Chem. Phys., 16, 11477-11496, doi:10.5194/acp-16-11477-2016, 2016.

Petters, M. D., and Wright, T. P. (2015), Revisiting ice nucleation from precipitation samples, *Geophys. Res. Lett.*, **42**, 8758–8766, doi:10.1002/ 2015GL065733.



Polen, M., Lawlis, E. and Sullivan, R. C.: The unstable ice nucleation properties of Snomax® bacterial particles, J. Geophys. Res. Atmos., 121(19), 11,666-11,678, doi:10.1002/2016JD025251, 2016.

Prenni, A. J., P. J. DeMott, D. C. Rogers, S. M. Kreidenweis, G. M. McFarquhar, G. Zhang, and M. R. Poellot, 2009: Ice nuclei characteristics from M-PACE and their relation to ice formation in clouds. Tellus, 61B, DOI: 10.1111/j.1600-0889.2009.00415.x, 436-448.

Price, H. C., Baustian, K. J., McQuaid, J. B., Blyth, A., Bower, K. N., Choularton, T., Cotton, R. J., Cui, Z. Field, P. R., Gallagher, M., Hawker, R., Merrington, A., Miltenberger, A., Neely, R. R. III, Parker, S. T., Rosenberg, P. D., Taylor, J. W., Trembath, J., Vergara-Temprado, J., Whale, T. F., Wilson, T. W., Young, G., and Murray, B. J.: Atmospheric ice nucleating particles in the dusty tropical Atlantic. Journal of Geophysical Research: Atmospheres, 123. https://doi.org/10.1002/2017JD027560, 2018.

Pummer, B. G., Bauer, H., Bernardi, J., Bleicher, S., and Grothe, H.: Suspendable macromolecules are responsible for ice nucleation activity of birch and conifer pollen, Atmos. Chem. Phys., 12, 2541-2550, doi:10.5194/acp-12-2541-2012, 2012.

Reicher, N., Segev, L., and Rudich, Y.: The WeIzmann Supercooled Droplets Observation (WISDOM) on a Microarray and application for ambient dust, Atmos. Meas. Tech. Discuss., https://doi.org/10.5194/amt-2017-172, accepted, 2017.

Rogers, D. C.: Development of a continuous flow thermal gradient diffusion chamber for ice nucleation studies, Atmospheric Research, *22*(2), 149-181, doi:10.1016/0169-8095(88)90005-1, 1988.

Rogers, D. C., P. J. DeMott, S. M. Kreidenweis and Y. Chen: A continuous flow diffusion chamber for airborne measurements of ice nuclei, J. Atmos. Oceanic Technol., 18, 725-741, doi:10.1175/1520-0426(2001)018<0725:ACFDCF>2.0.CO;2, 2001.

Santachiara, G., Di Matteo, L., Prodi, F., Belosi, F.: Atmospheric particles acting as Ice Forming Nuclei in different size ranges, Atmos. Res. 96, 266-272, 2010.

Schmitz, C. H. J., Rowat, A. C., Koster, S. and Weitz, D. A.: Dropspots: a picoliter array in a microfluidic device, Lab on a Chip, 9, 44–49, doi:10.1039/B809670H, 2009.

Schiebel, T., Höhler, K., Levin, E. J. T., Nadolny, J., Suski, K. J., Weber, I., DeMott, P. J., Leisner, T., and Möhler, O.: The new continuous flow diffusion chamber INKA for ice nucleation measurements, In preparation for submission to Atmos. Meas. Tech, Discuss., 2018.

Schill, G. P., Jathar, S. H., Kodros, J. K., Levin, E. J. T., Galang, A. M., Friedman, B., Link, M. F., Farmer, D. K., Pierce, J. R., Kreidenweis, S. M. and DeMott, P. J.: Ice-nucleating particle emissions from photochemically-aged diesel and biodiesel exhaust, Geophys. Res. Lett., 43, 5524–5531, doi:10.1002/2016GL069529, 2016.

Schnaiter, M., Büttner, S., Möhler, O., Skrotzki, J., Vragel, M., and Wagner, R.: Influence of particle size and shape on the backscattering linear depolarisation ratio of small ice crystals – cloud chamber measurements in the context of contrail and cirrus microphysics, Atmos. Chem. Phys., 12, 10465-10484, doi:10.5194/acp-12-10465-2012, 2012.



Schrod, J., Danielczok, A., Weber, D., Ebert, M., Thomson, E. S., and Bingemer, H. G.: Re-evaluating the Frankfurt isothermal static diffusion chamber for ice nucleation, Atmos. Meas. Tech., 9, 1313-1324, doi:10.5194/amt-9-1313-2016, 2016.

Steinke, I., Funk, R., Busse, J., Iturri, A., Kirchen, S., Leue, M., Möhler, O., Schwartz, T., Schnaiter, M., Sierau, B., Toprak, E., Ullrich, R., Ulrich, A., Hoose, C., and Leisner, T.: Ice nucleation activity of agricultural soil dust aerosols from Mongolia, Argentina, and Germany, J. Geophys. Res. Atmos., 121, 13,559-13,576, doi:10.1002/2016JD025160, 2016.

Stetzer, O., Baschek, B., Löünd, F., and Lohmann, U.: The Zurich Ice Nucleation Chamber (ZINC)—A new instrument to investigate atmospheric ice formation, Aerosol Sci. Technol., 42(1), 64–74, doi:10.1080/02786820701787944, 2008.

Tan, I., T. Storelvmo, and M. D. Zelinka, 2016: Observational constraints on mixed-phase clouds imply higher climate sensitivity, Science, 352 (6282), 224-227, doi:10.1126/science.aad5300.

Tobo, Y., P. J. DeMott, T. C. J. Hill, A. J. Prenni, N. G. Swoboda-Colberg, G. D. Franc, and S. M. Kreidenweis, 2014: Organic matter matters for ice nuclei of agricultural soil origin. Atmos. Chem. Phys. Discuss., 14, 9705–9728.

Vali, G.: Quantitative evaluation of experimental results on the heterogeneous freezing nucleation of supercooled liquids. J. Atmos. Sci., 28, 402–409, doi:10.1175/1520-0469(1971)028<0402:QEOERA>2.0.CO;2, 1971.

Vali, G., DeMott, P. J., Möhler, O., and Whale, T. F., Technical Note: A proposal for ice nucleation terminology, Atmos. Chem. Phys., 15, 10263–10270, doi:10.5194/acp-15-10263-2015, 2015.

Wagner, R., Möhler, O., Saathoff, H., Schnaiter, M., and Leisner, T.: New cloud chamber experiments on the heterogeneous ice nucleation ability of oxalic acid in the immersion mode, Atmos. Chem. Phys., 11, 2083–2110, doi:10.5194/acp-11-2083-2011, 2011.

Welti, A., Müller, K., Fleming, Z. L., and Stratmann, F.: Concentration and variability of ice nuclei in the subtropical maritime boundary layer, Atmos. Chem. Phys., 18, 5307-5320, https://doi.org/10.5194/acp-18-5307-2018, 2018.

Wex, H., Augustin-Bauditz, S., Boose, Y., Budke, C., Curtius, J., Diehl, K., Dreyer, A., Frank, F., Hartmann, S., Hiranuma, N., Jantsch, E., Kanji, Z. A., Kiselev, A., Koop, T., Möhler, O., Niedermeier, D., Nillius, B., Rösch, M., Rose, D., Schmidt, C., Steinke, I., and Stratmann, F.: Intercomparing different devices for the investigation of ice nucleating particles using Snomax® as test substance, Atmos. Chem. Phys., 15, 1463-1485, doi:10.5194/acp-15-1463-2015, 2015.

Whale, T. F., Murray, B. J., O'Sullivan, D., Wilson, T. W., Umo, N. S., Baustian, K. J., Atkinson, J. D., Workneh, D. A., and Morris, G. J.: A technique for quantifying heterogeneous ice nucleation in microlitre supercooled water droplets, Atmos. Meas. Tech., 8, 2437-2447, 2015

Whale, T. F., Holden, M. A., Kulak, A. N., Kim, Y.-Y., Meldrum, F. C., Christenson, H. K., and Murray, B. J.: The role of phase separation and related topography in the exceptional ice-nucleating ability of alkali feldspars, Phys. Chem. Chem. Phys., , 19, 31186—31193, doi: 10.1039/c7cp04898j, 2017.

Wright, T. P. and Petters, M. D.: The role of time in heterogeneous freezing nucleation, J. Geophys. Res. Atmos., 118, 3731–3743, doi:10.1002/jgrd.50365, 2013.



Yankofsky, S. A., Levin, Z., Bertold, T. Sandlerman, N.: Some basic characteristics of bacterial freezing nuclei, J. Appl. Meteor., 20, 1013-1019, 1981.

Zenker, J., Collier, K. N., Xu, G., Yang, P., Levin, E. J. T., Suski, K. J., DeMott, P. J., and Brooks, S. D., Using depolarization to quantify ice nucleating particle concentrations: a new method, Atmos. Meas. Tech., 10, 4639–4657, https://doi.org/10.5194/amt-10-4639-0, 2017.

Atmos. Meas. Tech. Discuss., https://doi.org/10.5194/amt-2018-191
Manuscript under review for journal Atmos. Meas. Tech.
Discussion started: 10 July 2018


Atmospheric Measurement Techniques Discussions

**Table 1.** Dry aerosol-based online INP instruments

| Instrument | Type | Institute | References |
|---|---|---|---|
| AIDA | Expansion cloud chamber | Karlsruhe Institute of Technology | Möhler et al. (2003); Möhler et al. (2005); Niemand et al. (2012) |
| CFDC-CSU | Continuous flow diffusion chamber (cylindrical) | Colorado State University | Rogers (1988); Rogers et al. (2001); Eidhammer et al. (2010) |
| CFDC-TAMU | Continuous flow diffusion chamber (cylindrical) | Texas A&M University | Glen and Brooks (2014); Zenker et al. (2017) |
| INKA | Continuous flow diffusion chamber (cylindrical) | Karlsruhe Institute of Technology | Schiebel et al. (2018) |
| SPIN-MIT | Continuous flow diffusion chamber (parallel) | Massachusetts Institute of Technology | Garimella et al. (2016) |
| SPIN-TROPOS | Continuous flow diffusion chamber (parallel) | Institute for Tropospheric Research | Garimella et al. (2016) |
| CIC-PNNL | Continuous flow diffusion chamber (parallel) | Pacific Northwest National Laboratory | Friedman et al. (2011) and Kulkarni et al. (2016) |
| PINC<br>PIMCA-PINC | Continuous flow diffusion chamber (parallel)<br>Immersion mode adaptation | ETH-Zurich | Chou et al. (2011); Kanji et al. (2013); Kohn et al. (2016) |

**Table 2.** Dry and wet suspension offline INP instruments

| Instrument | Type | Institute | References |
|---|---|---|---|
| NCSU-CS | Cold stage droplet freezing array | North Carolina State University | Wright and Petters (2013); Hader et al. (2014); Hiranuma et al. (2015). |
| CMU-CS | Cold stage droplet freezing array in oil | Carnegie Mellon University | Polen et al. (2016); Beydoun et al. (2017) |
| KIT-CS | Cold stage droplet freezing array in oil | Karlsruhe Institute of Technology | Peckhaus et al. (2016) |
| µL-NIPI | Cold stage droplet freezing array | University of Leeds | Whale et al. (2015) |
| BINARY | Cold stage droplet freezing array in compartments | Bielefeld University | Budke and Koop (2015) |
| IS | Aliquot array freezing | Colorado State University | Hiranuma et al. (2015); Hill et al. (2016) |
| VODCA | Cold stage emulsion freezing | Technical University of Vienna | Pummer et al. (2012) |
| WISDOM | Microfluidics droplet freezing train | Weizmann Institute | Reicher et al. (2017) |
| M-AL | Acoustic levitator | University of Mainz | Diehl et al. (2014) |
| FRIDGE-STD | Low pressure diffusion chamber (Si wafers) | Goethe University of Frankfurt | Klein et al. (2010); Schrod et al. (2016) |
| FRIDGE-IMM | Cold stage droplet freezing array (on wafers) | Goethe University of Frankfurt | Hiranuma et al. (2015) |
| DFPC-ISAC | Dynamic filter processing chamber | ISAC-CNR | Santachiara et al. (2010); Belosi et al. (2014) |

Atmos. Meas. Tech. Discuss., https://doi.org/10.5194/amt-2018-191
Manuscript under review for journal Atmos. Meas. Tech.
Discussion started: 10 July 2018


Atmospheric Measurement Techniques Discussions

**Table 3.** List of aerosol types, particle generation techniques and aerosol properties.

| Aerosol type[†] | Generator | AIDA Expt. ID | APC Expt. ID | BET specific sfc. ($m^2 g^{-1}$)[*] | Density ($g cm^{-3}$)[**] | Dynamic Shape Factor[**] | Reference[§] |
|---|---|---|---|---|---|---|---|
| Illite NX (IS03) | Rotating brush (PALAS, RGB1000) | FIN02_4,10, 22,25 | APC_1-4,7-8 | 124.4 | 2.6 | 1.3 | Hiranuma et al. (2015) |
| Argentinian soil dust (SDAr01) | Rotating brush (PALAS, RGB1000) | FIN02_5,9,24,26 | APC_9-10,20-21,29 | 13.1 | 2.6 | 1.2 | Steinke et al. (2016) |
| Saharan desert dust (SD6) | Rotating brush (PALAS, RGB1000) | FIN02_3 | APC_5-6 | 6.9 | 2.6 | 1.2 | Niemand et al. (2012) |
| Tunisian soil dust (SDT01) | Rotating brush (PALAS, RGB1000) | FIN02_7,12 | APC_11-12,27 | 7.0 | 2.6 | 1.2 | Lafon et al. (2006); Di Biagio et al. (2014) |
| K-rich feldspar (FS02) BCS376 | Rotating brush (PALAS, RGB1000) | FIN02_8,11, 14 | APC_13-14 | 2.6 | 2.6 | 1.1 | Atkinson et al. (2013); Peckaus et al. (2016) |
| Snomax (SM04) | Atomizer (TSI, 3076) | FIN02_6,13, 27 | APC_15-16,18-19,28 | N/A | 1.4 | 1.1 | Wex et al. (2015) |

[†]IDs in parentheses represent the AIDA-INUIT code names.

[*]The BET method to measure specific surface area of bulk powder is described in Hiranuma et al. (2014a). Note that our measurements have ± 5% uncertainty.

[**]For our geometric surface area estimations, we used the optimized effective densities and dynamic shape factors provided in this table.

[§]Bulk composition data of aerosols are available in these references. For SD6 and SDT01, XRD data are available upon request.

Atmos. Meas. Tech. Discuss., https://doi.org/10.5194/amt-2018-191
Manuscript under review for journal Atmos. Meas. Tech.
Discussion started: 10 July 2018


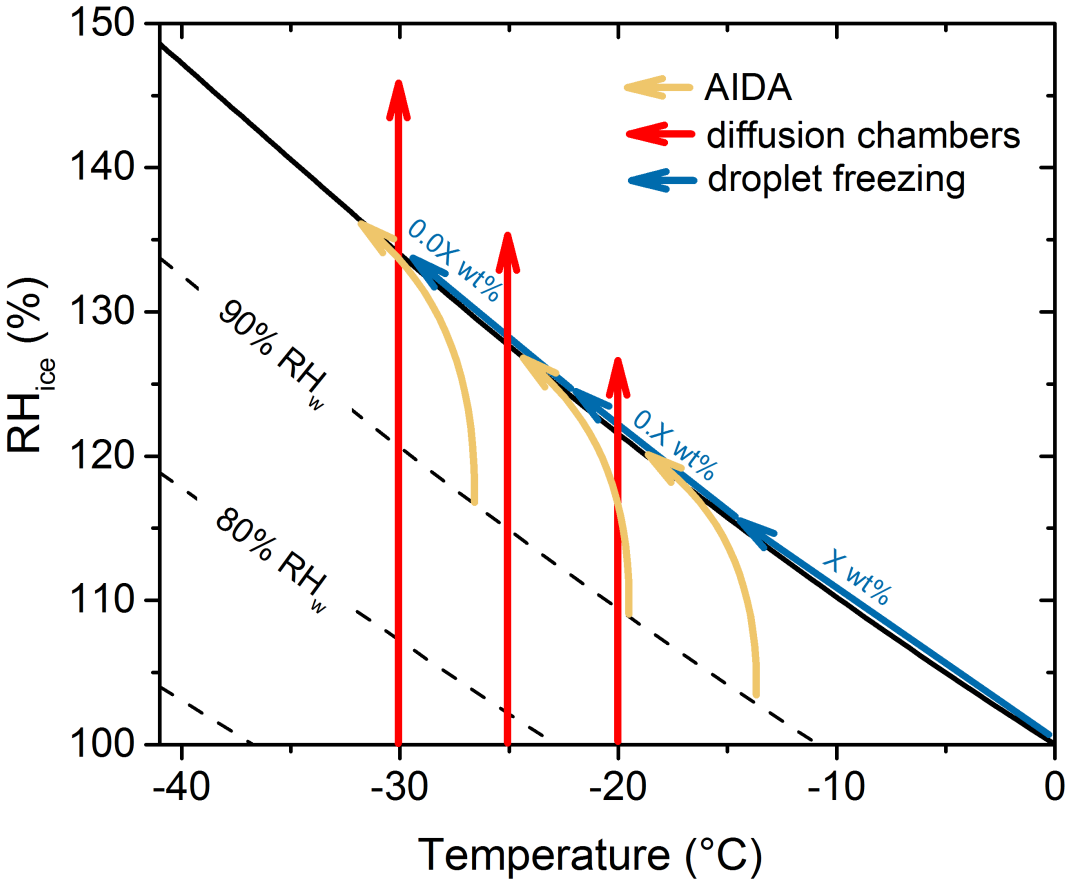


**Figure 1.** Schematic representation of different experiments conducted in the mixed-phase cloud temperature regime using different measurement systems during FIN-02. Yellow curves and arrows show the typical thermodynamic path of AIDA cloud chamber experiments. Red lines with arrows indicate the typical trajectory of online, continuous flow instrument systems and offline systems that process initially dry particle populations under controlled humidity and temperature conditions. The blue arrow following the water saturation line in T-RH$_w$ space shows the trajectory of subsequently diluted samples of X, 0.X an 0.0X weight percent suspensions of collected aerosols measured by immersion freezing methods. The PIMCA-PINC instrument follows the trajectory of the offline immersion freezing devices, but does so for water droplets activated originally on single dry aerosol particles (and hence without the varied weight percent).

Atmos. Meas. Tech. Discuss., https://doi.org/10.5194/amt-2018-191
Manuscript under review for journal Atmos. Meas. Tech.
Discussion started: 10 July 2018


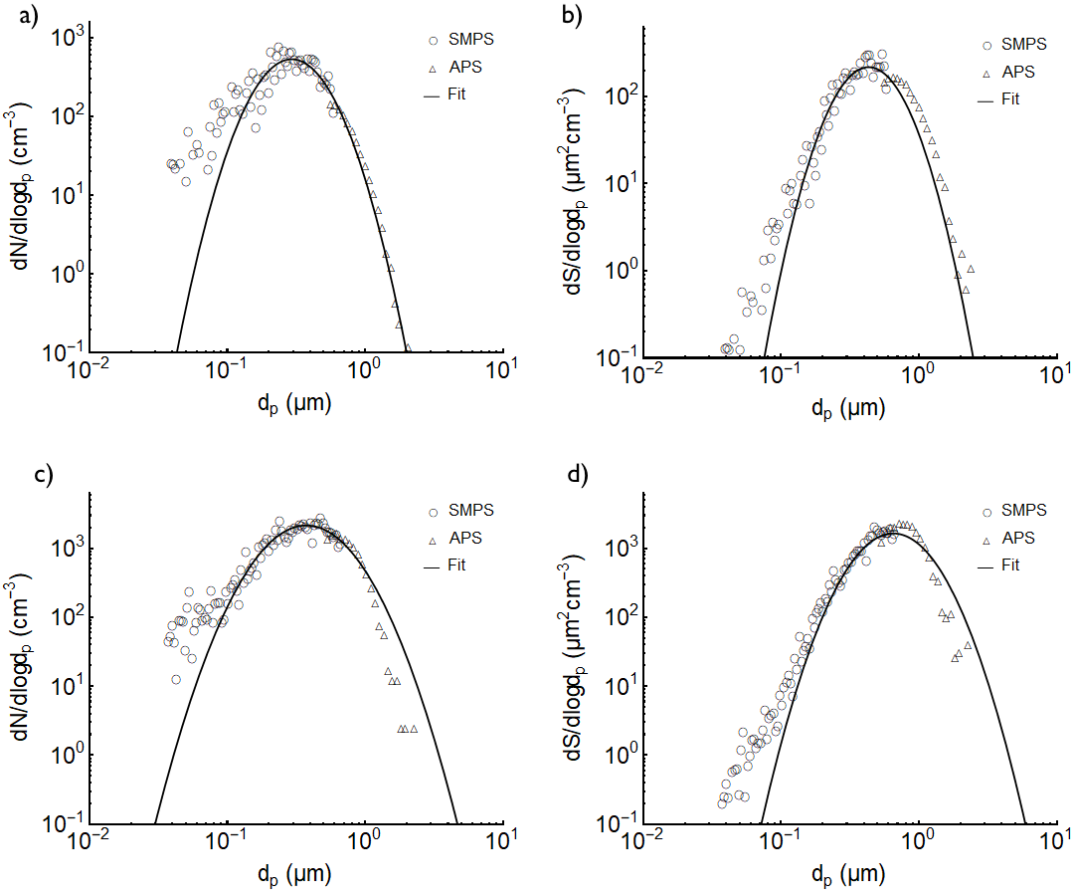


**Figure 2.** Number, in a), and surface area distribution, in b), of SDT01 dust particles generated into the AIDA chamber, measured with the SMPS and APS instruments, as well as the lognormal fits to the size distributions for exemplary AIDA experiment 12 on March 20, 2015, 648 s prior to expansion start. APS data have been converted based on assumed density (2.6 g cm$^{-3}$) and dynamic shape factor (1.2). The same data for SDT01 particles generated in APC experiment 12 on March 18, 2015, 785s following aerosol particle injection, are shown in panels c) and d). Lognormal fits are used to obtain total surface areas and these were tabulated as a function of time in each experiment.

Atmos. Meas. Tech. Discuss., https://doi.org/10.5194/amt-2018-191
Manuscript under review for journal Atmos. Meas. Tech.
Discussion started: 10 July 2018


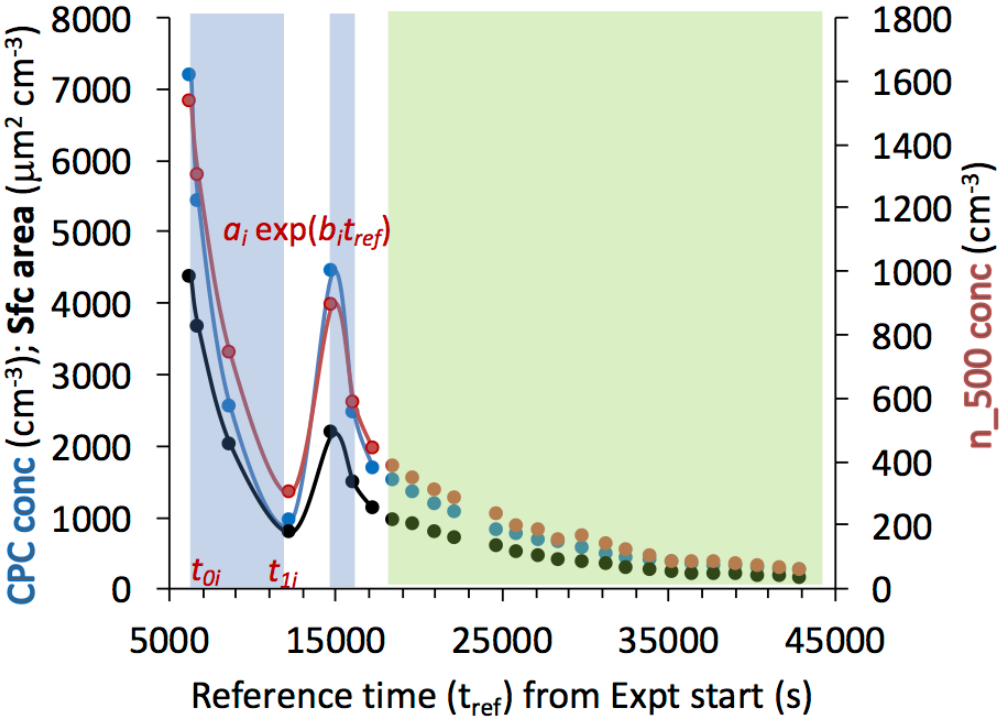


**Figure 3**. First half of a daily experimental series, after an initial fill of Tunisian soil dust (Experiment 11 and 12 of the FIN-02 APC series on March 18, 2015) into the APC at a time taken to be the experimental start time. Impinger and filter sample periods after the fill are highlighted in light blue, indicating that a refill was required on this day. To obtain a reference aerosol concentration ($cm^{-3}$) via the CPC (total particles) or optical particle counter at sizes larger than 500 nm (n_500), as well as surface area ($\mu m^2$ $cm^{-3}$) for the offline sampling period, the time-weighted average of the two sampling periods was determined. This concentration value could then be used to ratio versus the concentrations present at later sampling times during the online sampling of aerosols from the APC (green shaded region) in order to back-correct the online INP number concentrations to those interpreted from the offline samples.

Atmos. Meas. Tech. Discuss., https://doi.org/10.5194/amt-2018-191
Manuscript under review for journal Atmos. Meas. Tech.
Discussion started: 10 July 2018


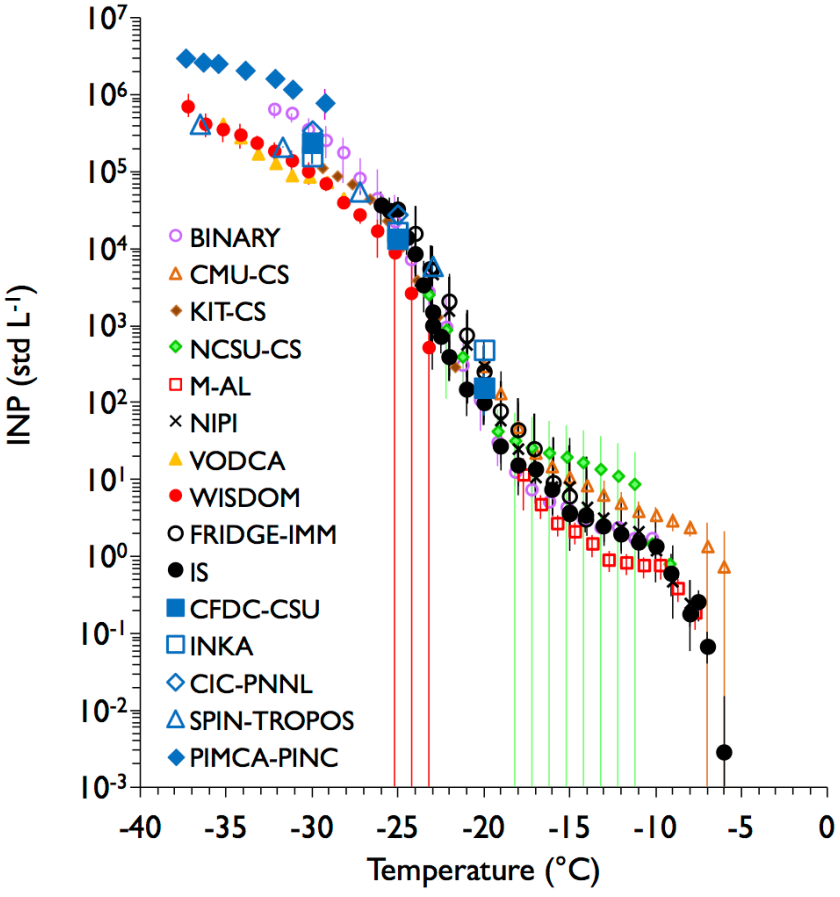


**Figure 4.** Combined results of all online and offline measurements of Argentinian soil dust sampled from the APC under conditions representative of those favoring immersion freezing nucleation in all devices. Note that most of the offline immersion freezing data have been sub-sampled at ~1°C intervals. These offline, bulk immersion freezing methods are distinguishable here by their smaller data points (using different symbols and colors) over a broad range of temperatures, whereas online methods using conditions supersaturated with respect to water (immersion freezing assumed as a major contributor) at specific temperatures are indicated by sparse (larger) blue data points. The KIT-CS, NCSU-CS, NIPI, VODCA, M-AL, BINARY and WISDOM instruments shared impinger samples, while the IS and FRIDGE-IMM used separate filter collections (distinguished here by black circle data points). As discussed in the text and Eqs. (1) - (3), corrections have been applied to online instrument data depending on the time of sampling, constituting a ratio of total particle concentrations present at the time of sampling offline impingers/filters to those present at the time of specific online measurements. Error bars represent 95% confidence intervals, unless stated otherwise in the Supplement. When error bars are not present on some points, they may be buried within the marker (small errors) or the binned point represents a single observation. The data herein correspond to FIN-02 APC experiments 9 and 10 on March 17, 2015.

Atmos. Meas. Tech. Discuss., https://doi.org/10.5194/amt-2018-191
Manuscript under review for journal Atmos. Meas. Tech.
Discussion started: 10 July 2018


Atmospheric Measurement Techniques Discussions

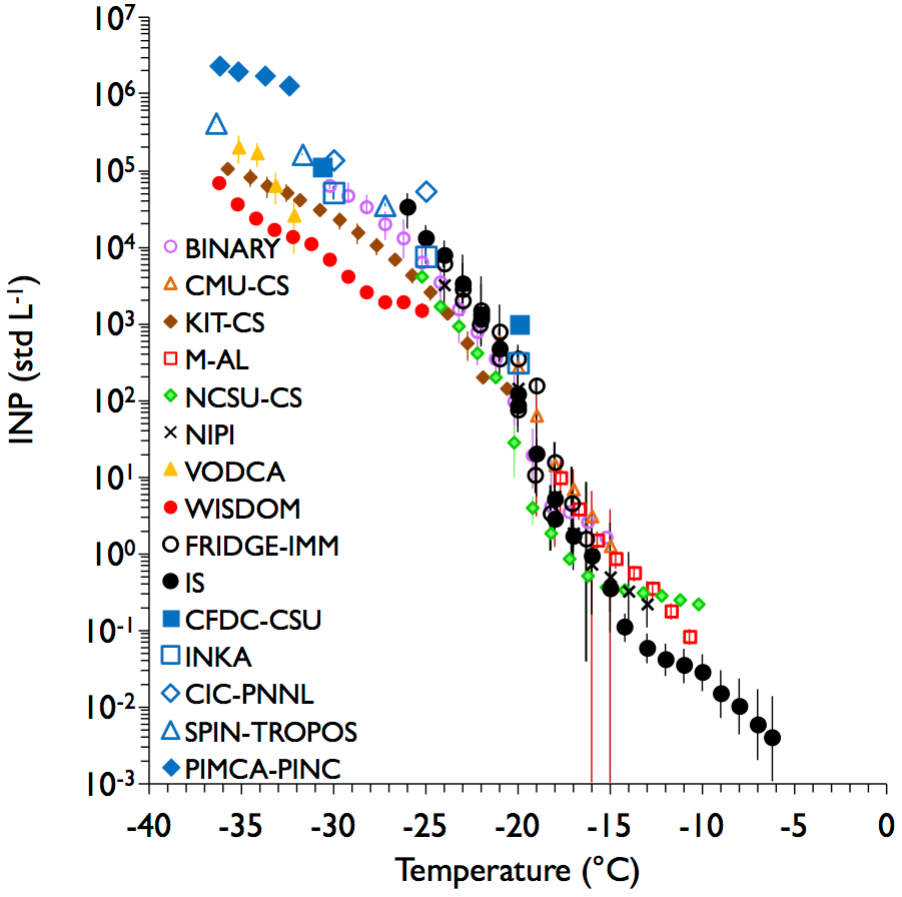


**Figure 5.** As in Fig. 4, but for sampling of Tunisian soil dust from the APC. All distinguishing features discussed with regard to Fig. 4 apply here as well. Note that two FRIDGE-IMM filter samples are represented here as two data points at a given temperature. The data herein correspond to FIN-02 APC experiments 11 and 12 on March 18, 2015.

Atmos. Meas. Tech. Discuss., https://doi.org/10.5194/amt-2018-191
Manuscript under review for journal Atmos. Meas. Tech.
Discussion started: 10 July 2018


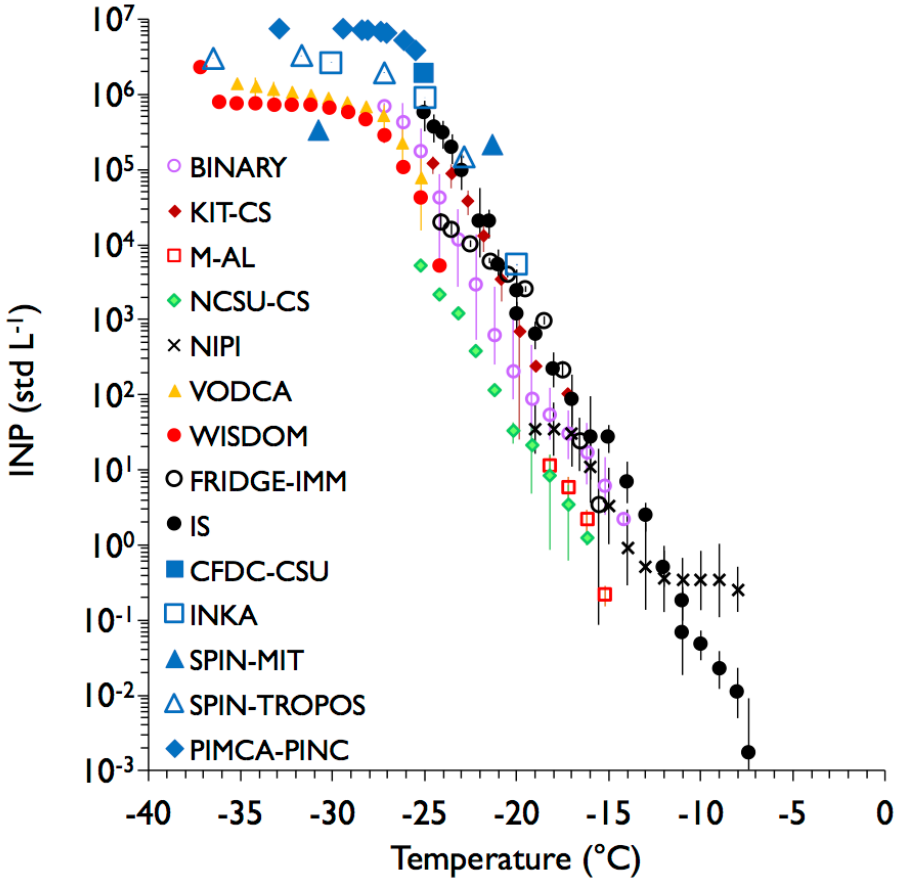


**Figure 6.** As in Fig. 4, but for sampling of K-feldspar particles from the APC. All distinguishing features discussed with regard to Fig. 4 apply here as well. The data herein correspond to FIN-02 APC experiments 13 and 14 on March 19, 2015.

Atmos. Meas. Tech. Discuss., https://doi.org/10.5194/amt-2018-191
Manuscript under review for journal Atmos. Meas. Tech.
Discussion started: 10 July 2018


Atmospheric Measurement Techniques Discussions

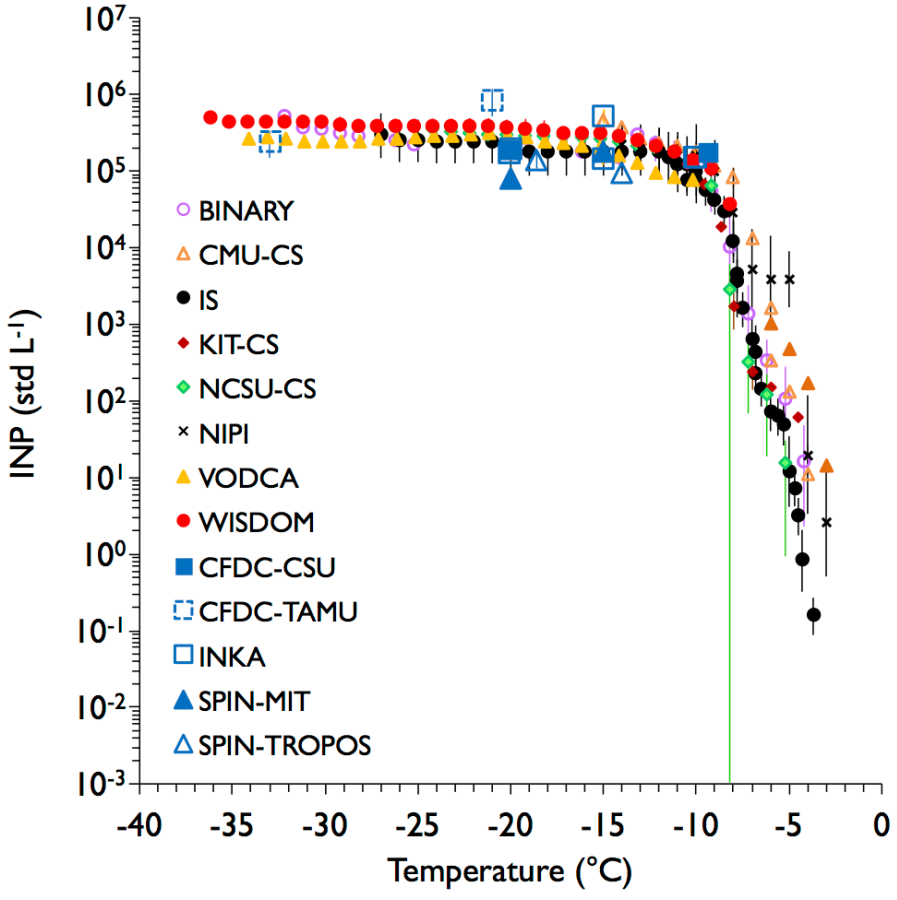


**Figure 7.** As in Fig. 4, but for sampling of aerosolized Snomax® particles from the APC. Two sets of measurements are plotted separately from the CMU-CS system (open and filled) due to variability observed between replicate samples as discussed in the text. The closed orange triangles are from experiments run immediately after the sample had thawed, while the open triangles are for runs that occurred within a few hours of thawing. All offline samplers processed data from the impinger samples in this case. INKA data are included for all water supersaturated conditions not exceeding water breakthrough $RH_w$. The data herein correspond to FIN-02 APC experiments 15 and 16 on March 20, 2015.

Atmos. Meas. Tech. Discuss., https://doi.org/10.5194/amt-2018-191
Manuscript under review for journal Atmos. Meas. Tech.
Discussion started: 10 July 2018


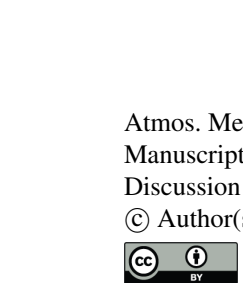

Atmospheric Measurement Techniques Discussions

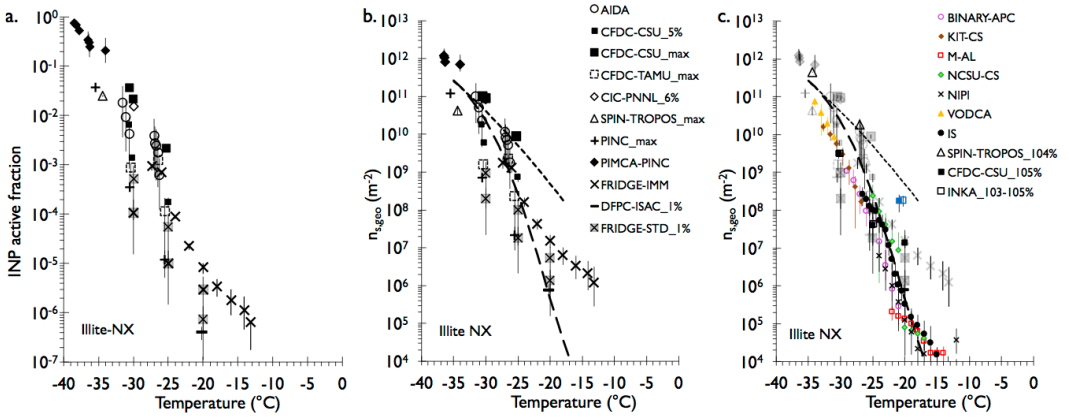


**Figure 8.** Panel a: Ice active fraction from multiple experiments performed on illite NX aerosols sampled directly from the AIDA chamber prior to expansion cloud experiments. In these cases, the subsequent AIDA measurements of activated ice crystal concentrations are included for comparison when water supersaturation was achieved during the expansion cycle. Instrument symbols are shown in Panel b. Panel b: Conversion of data to geometric surface active site density parameter, $n_{s,geo}$ using AIDA aerosol distribution data, and data within Table 3. Where specific instrument water supersaturations were selected for comparison, these are indicated after the instrument label (e.g., CIC-PNNL_6%, implies 106% $RH_w$). The term "max" means the highest $RH_w$ achieved in a scan (102-110%), as listed in Table S1. FIN-02 AIDA experiments (unnumbered, March 11, 2015), 4 (March 16, 2015), 10 (March 19, 2015), 22 (March 26, 2015), and 25 (March 27, 2015) are represented. Gumbel cumulative distribution (log-space) fit curves for illite NX are from Hiranuma et al. (2015; cf., Table 3), representing wet suspension (long dash) and dry-dispersion experiments (short dash) in that study. Panel c: Wet suspension (colored points) and flow chamber (black points) $n_{s,geo}$ data derived from APC experiment 7 (March 16, 2015) for all instruments listed in the legend are overlain on greyed-out AIDA experiment points from Panel b. Additional CFDC-CSU and INKA data points from APC experiment 3 (March 13, 2015) are included as blue data points for these instruments

Atmos. Meas. Tech. Discuss., https://doi.org/10.5194/amt-2018-191
Manuscript under review for journal Atmos. Meas. Tech.
Discussion started: 10 July 2018


Atmospheric Measurement Techniques Discussions

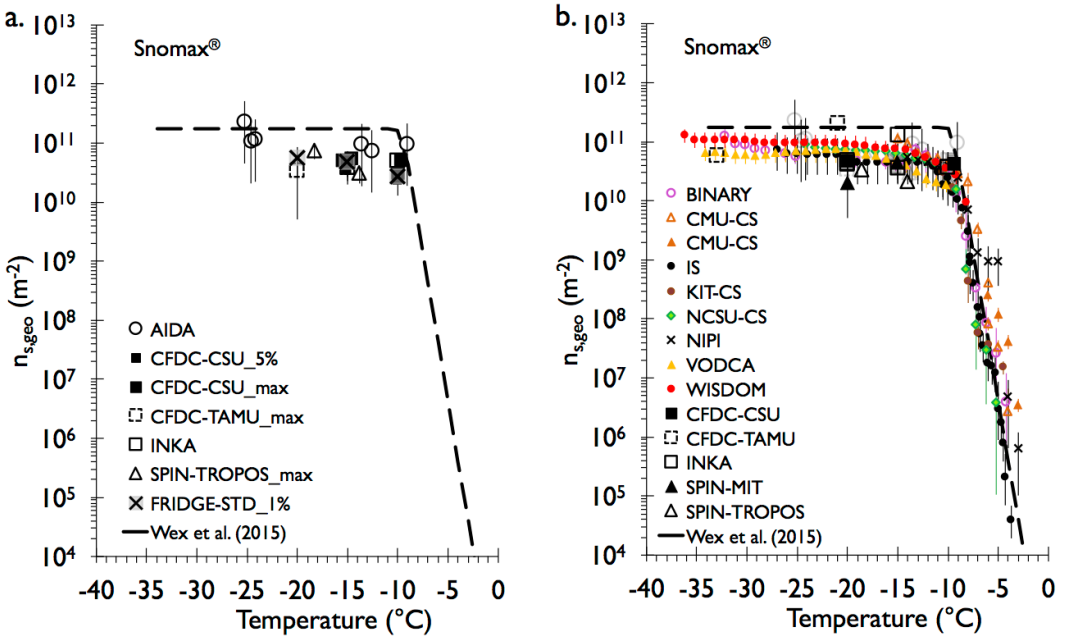


**Figure 9.** As in Fig. 8. Panel a: Ice active site density in multiple experiments performed on Snomax® aerosols sampled directly from the AIDA chamber. AIDA experiments 6 (March 17, 2015) and 13 (March 21, 2015) are represented, as listed for different instruments in Tables S1 and S2. The fit for $n_{s,geo}$ is derived from the Wex et al. (2015) fit for nm, the number of molecular INPs per dry mass of Snomax®, as explained in the text. Panel b: $n_{s,geo}$ derived from FIN-02 APC experiments 15 and 16 on March 20, 2015 (Fig. 7) are overlain on greyed-out AIDA experiment data points from Panel a.

Atmos. Meas. Tech. Discuss., https://doi.org/10.5194/amt-2018-191
Manuscript under review for journal Atmos. Meas. Tech.
Discussion started: 10 July 2018




Atmospheric Measurement Techniques Discussions

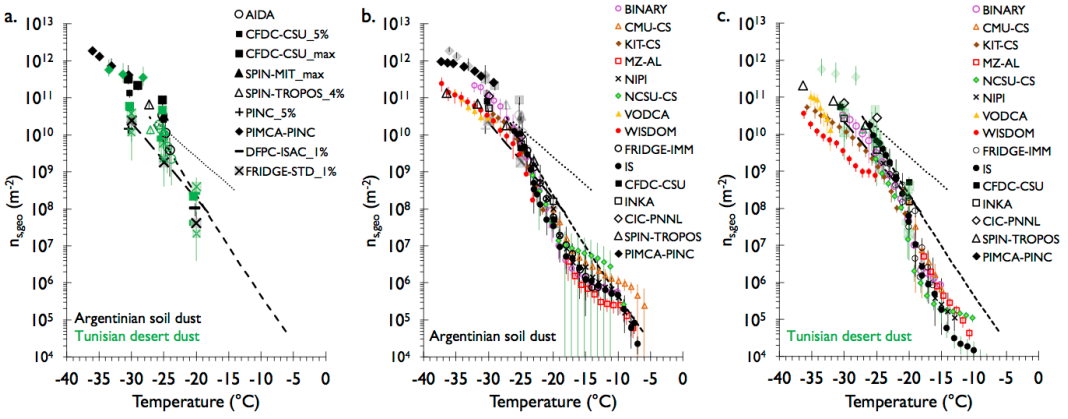


**Figure 10.** As in Figures 8 and 9, but for Argentinian soil dust and Tunisian soil dust sample experiments. Panel a: Data from FIN-02 AIDA experiments 5 (March 16, 2015), 9 (March 19, 2015), 24 (March 26, 2015), and 26 (March 27, 2015) are represented for Argentinian soil dust, and AIDA experiments 7 (March 18, 2015) and 12 (March 20, 2015) are represented for Tunisian soil dust, as listed for different instruments in Table S1. AIDA cloud expansion results are represented only for AIDA experiments 7 and 9, when mixed-phase clouds formed and persisted. Two fits of $n_{s,geo}$ *(T)* for previous surface soil dust particle types reported in the literature are from Tobo et al. (2014) ("Wyoming soil dust", long-dashed) and O'Sullivan et al. (2014) ("fertile soil dust", short-dashed), and Steinke et al. (2016) ("agricultural soil dust", dotted). APC data from Fig. 4 for Argentinian dust and Fig. 5 for Tunisian dust are overlain in panels b and c, respectively.

Atmos. Meas. Tech. Discuss., https://doi.org/10.5194/amt-2018-191
Manuscript under review for journal Atmos. Meas. Tech.
Discussion started: 10 July 2018


Atmospheric Measurement Techniques Discussions

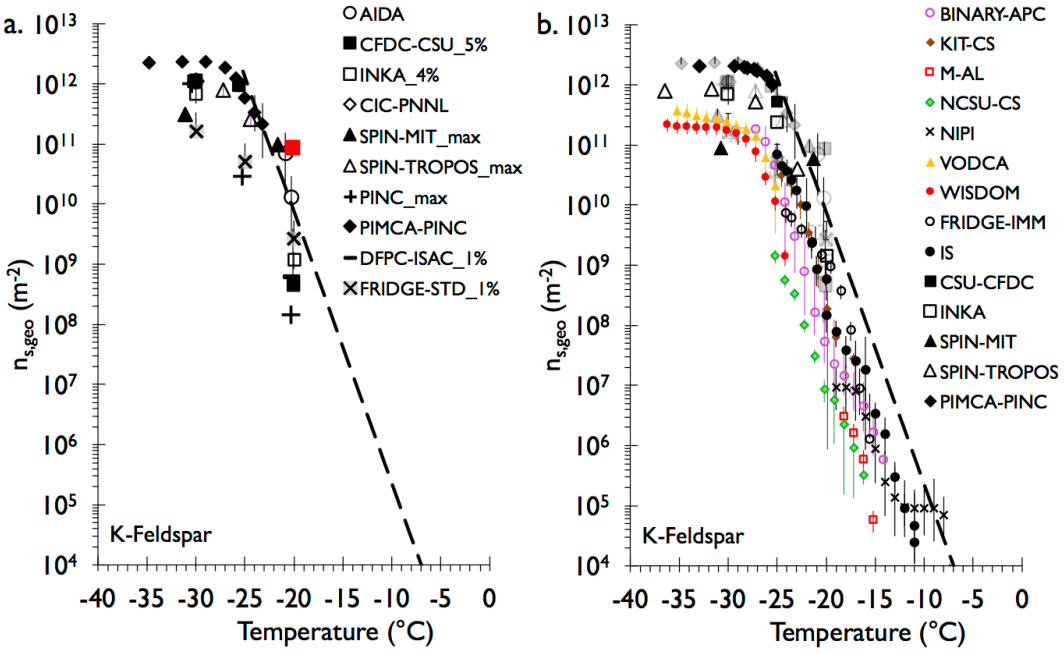


**Figure 11.** As in Fig. 9, but for K-feldspar aerosols sampled from the AIDA chamber prior to expansion-cooling experiments 8 (March 18, 2015), 11 (March 201, 2013), and 14 (March 23, 2013) for panel a, and overlay of data from APC experiments 13 and 14 on March 19, 2015 (Fig. 6) in panel b. The K-feldspar fit from Atkinson et al. (2013) is shown for comparison, after conversion from $n_{s,BET}$ to $n_{s,geo}$, as described in the text. The experiment represented by the red data point in panel a from the CFDC-CSU instrument is discussed in Supplement Section S.1.2 in relation to experimental detection issues.